Chair of Petroleum and Geothermal Energy Recovery

Master Thesis

GOHFER® Software Evaluation

Written by:
Dipl.-Ing. Albina Mukhamedzianova

Advisor:
Dipl.-Ing. Dipl.-Ing. Dr.mont. Clemens Langbauer

Leoben, 20.09.2017

EIDESSTATTLICHE ERKLÄRUNG

Ich erkläre an Eides statt, dass ich die vorliegende Diplomarbeit selbständig und ohne fremde Hilfe verfasst, andere als die angegebenen Quellen und Hilfsmittel nicht benutzt und die den benutzten Quellen wörtlich und inhaltlich entnommenen Stellen als solche erkenntlich gemacht habe.

AFFIDAVIT

I hereby declare that the content of this work is my own composition and has not been submitted previously for any higher degree. All extracts have been distinguished using quoted references and all information sources have been acknowledged.

Danksagung / Acknowledgement

Optional.

Kurzfassung

In dieser Master Thesis wird das Potential der “Bio Enhanced Energy Recovery” (BEER ®) Hydraulic Fracturing Technologie in sehr gering permeablen Sandsteingaslagerstätten unter Verwendung der 3D-Simulationssoftware GOHFER® behandelt. Untersucht wird nicht nur das Fließverhalten unterschiedlicher Flüssigkeiten, sondern auch die Effektivität in der Interaktion mit Glaskugeln als Proppants. Diese Resultate werden mit gängigen Produkten verglichen.

Heutzutage gibt es eine große Nachfrage nach neuen umweltfreundlichen Produkten, welche einerseits umweltverträglich und andererseits anwendungstechnisch effektiv sind.

Diese Master Thesis setzt sich aus zwei Teilen zusammen: Experimente und Simulationen. Der experimentelle Teil dieser Arbeit beinhaltet rheologische Tests der BEER® Flüssigkeit und Filteranalysen der Glaskugeln. Der Simulationsteil untersucht die Lagerstätteneigenschaften, die Planung der Hydraulic Fracturing Behandlung, die 3D-Rissgeometrie und evaluiert die Verbesserung der Produktion nach der Behandlung. Zusätzlich wurde eine Sensitivitätsanalyse durchgeführt, um die Länge der Rissbilung, die Ausbreitung der Proppants, die Leitfähigkeit und Produktionsraten in Bezug auf verschiedene Parameter, wie Proppants Materialien, den Umfang des Verfahrens und Flüssigkeitsraten zu untersuchen.

Die Ergebnisse der Simulationen zeigen, dass die BEER® Hydraulic Fracturing Technologie für die untersuchte Lagerstätte geeignet ist. Sie liefert sowohl eine gute Rissgeometrie, als auch eine Produktionssteigerung. Außerdem wurde bestätigt, dass GOHFER® benutzerdefinierte Hydraulic Fracturing Simulationen ermöglicht. Zusätzlich wurde nachgewiesen, dass der Software Algorithmus sehr genaue Resultate für limitierte Testdaten liefert.

Abstract

This thesis evaluates the potential of Bio Enhanced Energy Recovery (BEER®) technology application in the tight gas sandstone reservoir hydraulic fracturing job with the help of the 3D simulator GOHFER®. The fluid rheology is investigated and, furthermore, efficiency of the fluid and glass beads proppants application is evaluated and compared to the common commercially available products.

Nowadays, there is a great demand for the new eco-friendly products that would be compatible with the environment, on the one hand, and would be efficient in terms of its technical application, on the other hand.

The thesis consists of two parts: experiments and simulations. The experimental part of this work includes rheological tests performed for the BEER® fluid and sieve analysis performed for the glass beads. The simulation part consists of analyzing the reservoir properties, designing the treatment job, investigating the 3D fracture geometry and post-treatment production enhancement evaluation. In addition, the sensitivity analysis is performed in order to investigate the gross fracture length, the propped fracture cutoff length, conductivity and production rates behavior depending on different variables, such as proppant materials, job treatment size and slurry rates.

The results obtained by the simulation indicate, that the proposed technology is indeed suitable for hydraulic fracturing treatment of the analyzed reservoir and that it provides good fracture geometry, as well as the production improvement. Moreover, it has been confirmed that GOHFER® allows to model a user defined fracturing fluid, as well as proppants. In addition, it has been proved that the software calculation algorithm is based on the rigorous studies of the hydraulic fracturing processes and therefore gives very accurate results.

Table of content

Page

1 Introduction

The main purpose of hydraulic fracturing stimulation is to increase ultimate recovery and to postpone an economic limit of the well. In order to enhance the natural connection of the wellbore with the reservoir, a conductive channel is created and extended to a certain reservoir depth. This is achieved by pumping special hydraulic fluids at high pressure and rate into the reservoir intervals, causing the fracture to open. The proppants are mixed with the fluids and keep the fracture in open position upon treatment completion.

In order to design an optimum hydraulic fracturing treatment, an engineer must correlate different types of data. Based on available data, the optimum fracture parameters are identified, the most suitable fracturing fluid and proppants both in terms of efficiency and economic considerations are selected and the simulation is performed in the special fracturing simulation software. The efficiency of the treatment is evaluated based on the post-treatment production analysis.

1.1 Problem definition

In order to meet the complex energy demands, on the one hand, and to enhance the public acceptance of expanding oil and gas industry activity, on the other hand, petroleum companies must aim to perform their operations safe, with zero incidents and with the minimum environmental impact.

Hydraulic fracturing treatment imposes big concerns among public for the possibility of the chemical contamination of drinking fluid by spills, below ground liquids and gases migration and inadequate treatment.

Due to these reasons, there as a great demand for the industry to develop new environmentally friendly technologies, implement proper policies and practices and, therefore, to reduce the environmental footprint caused by hydraulic fracturing treatment. The innovative hydraulic fracturing fluid BEER®, developed by Montanuniversitaet Leoben, consists of the fully environmentally compatible components and therefore is in full compliance with the industry demands.

1.2 Objective

The objective of this Master Thesis is to investigate efficiency of the BEER® fluid and glass beads, used for hydraulic fracturing treatment simulation in the GOHFER® software. The experimental part of this work includes rheological tests on the fluid and glass beads. The simulation part includes modelling the fluid rheology in the software, developing the optimum pumping schedule for the treatment, obtaining the 3D fracture geometry and evaluating post-treatment production enhancement.

2 Literature review

Due to the fact that this thesis is focused on the hydraulic fracturing treatment, the basics of the fracturing process, the operations sequence as well as design procedure are described in this chapter. The chapter starts with identification of the main objective of the hydraulic fracturing treatment, then it considers the most important formation evaluation parameters that influence the efficient design and execution of the treatment process, the design steps and lastly it describes the available commercial 3D fracturing softwares with the specific focus on GOHFER® software.

2.1 Hydraulic fracturing basics

Hydraulic fracturing is the process of creating a fracture or fracture system in the porous media by pumping specially designed fluids into a wellbore at pressures that exceed the fracture pressure, leading to formation breaking. The effectiveness of hydraulic fracturing treatment is measured by fracture orientation, fracture system extent and by post fracture enhancement of gas and liquid recovery.

The purpose of the hydraulic fracturing treatment is to increase the productivity index of the producing well. The productivity index defines the volume of oil or gas that can be produced at a given pressure differential between the reservoir and the wellbore.

The geometry of propagating fractures is governed by rock mechanics aspects. The important mechanical properties for treatment design and analysis are: elastic properties (Young's and shear modulus, Poisson's ratio); strength properties (fracture toughness, tensile and compressive strength); ductility; friction; poroelastic parameters. However, the most important parameter for overall fracture design is in-situ stress field.

The size and orientation of a fracture, and the magnitude of the pressure needed to create it, are dictated by the formations in situ stress field. This stress field is defined by three principal compressive stresses, oriented perpendicular to each other. The principal compressive stresses are a vertical stress (σ_v), a maximum and minimum horizontal stress (σ_{hmax} and σ_{hmin}). These stresses are depicted in Figure 1 with red arrows. Tectonic regime in the region, depth, pore pressure and rock properties determine how stress is transmitted among formations.

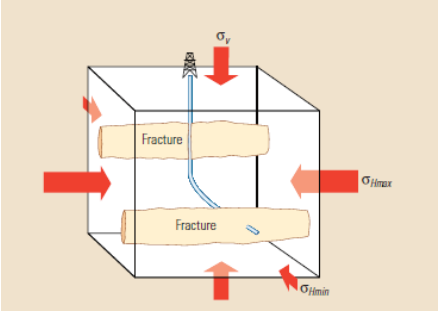

Figure 1: Vertical Fracture propagation [1, p. 51]

Hydraulic fractures may be defined as pressure-induced tensile fractures, and they open in the direction of the least resistance. If the maximum principal compressive stress is the overburden stress, like it is depicted in Figure 1, then the plane of the fracture will be vertical, propagating perpendicular to the minimum horizontal stress and parallel to the maximum horizontal stress. In some cases, however, the overburden stress is the least principal stress, thus, the hydraulic fracture will be horizontal.

Minimum stress may be determined from leak-off test (LOT), extended leak-off test (XLOT) or by the mini-frac post treatment data. LOT and XLOT are preferred over formation integrity test (FIT), since they give more reliable data.

Understanding the distribution of the stresses is critical for the evaluation of the fracture growth, geometry and treating pressures. Stress distributions control fracture orientation, height containment, treating pressures magnitude and change in treating pressure during the job. The magnitude of the minimum stress determines the fluid pressure required to open a fracture.

During fracture initiation, the fluid is pumped down the wellbore at the pressure high enough to overcome leak-off into the permeable zone. At this stage the injection achieves the radial flow, therefore, fluid leak-off is relatively low. The more fracture continues to propagate, the more fracturing fluid is leaking off to the formation. Therefore, the higher leak-off is associated with the longer fractures, especially in cases, when the fracture fluids do not build up a filter cake on the fracture wall. Figure 2 represents the parameters that control the leak-off.

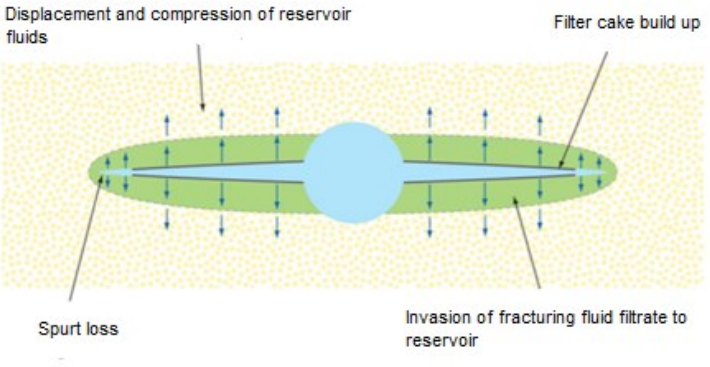

Figure 2: Fracture propagation and leak-off control [2, p. 84]

The fracturing fluid displaces or compresses the reservoir fluid. Gas reservoirs are easier to compress and have a lower viscosity, promoting therefore, a higher leak-off. The further the fracturing fluid filtrate is invading and displacing the reservoir fluid, the more pressure difference through the invaded zone will be created due to the fluid viscosity and relative permeability. That is why the fluids with the capability to maintain their viscosity (fluids with polymers) will reduce leak-off. Prior to the generation of the effective filter cake, there will be an additional fluid loss, which is termed as spurt loss. As some point, the external filer cake

will stop growing, once equilibrium between the flow through the filter cake and erosion of the filter cake is reached.

The leak-off parameters are critical to designing a fracture treatment, therefore, generally, mini-fracs (or datafracs) are performed prior to the main treatment in order to reduce the uncertainty in these parameters and determine the minimum stress without committing to placing proppants down the wellbore.

The leak-off coefficient is a measure of leak-off velocity at any point along the fracture face, accounting for the time the fracture has been exposed. The leak-off coefficient depends on the formation permeability, the fracture area, the pressure differential between the fracturing fluid and the formation. Low efficiency fluid provides higher leak-off rates. The leak-off coefficient defines the volume of fluid leaked off into the formation by **Eq.1**:

$$V_l = \pi * C_{eff} * \mathrm{A} * \sqrt{t} \qquad (1)$$

V_i volume of fluid leaked off into formation [ft^3]
C_{eff} fluid leak-off coefficient [$ft/min^{1/2}$]
A surface area of the fracture [ft^2]
t the time that the fracture was open [min]

The efficiency (e) of the fluid use can be determined by **Eq.2**:

$$E = \frac{V_l}{V_t} \qquad (2)$$

E fluid efficiency [frac]
V_i volume of fluid leaked off into formation [ft^3]
V_t total volume of fluid pumped into formation [ft^3]

There is a certain limit to how far the fracture can propagate, for instance, low permeability reservoirs benefit from longer fractures than higher permeability ones. The leak-off in low permeability reservoirs is reduced.

In addition, the deeper fracture propagates, the higher will be the frictional pressure along the fracture, which will create a higher treating pressure, and therefore, upward or downward growth of the fracture, as well as possible activation of higher stress intervals. High pressure leads to elastic deformation (strain) of the rock away from the fracture face; this deformation will depend on the pressure above the fracture pressure (called net pressure) and Young's modulus of the rock (modulus of elasticity). Greater deformation (i.e. wider fracture) will be created by higher net pressure and more elastic rocks.

Besides creating a fracture with the specific geometry, it is vital for the fracture to be conductive and productive. For that purpose, the fracture must be propped to ensure conductivity. This is generally achieved by pumping proppant in increasing concentrations down the wellbore.

In order to understand hydraulic fracturing, it is vital to differentiate between different terms of pressures. The main pressures used in hydraulic fracturing treatment are represented in Table 1.

Table 1: Pressure terms [3, pp. 5-6]

Pressure name	**Definition**
Closure pressure, P_c	This is the pressure acting to close the fracture. Below this pressure the fracture is closed, above this pressure the fracture is open. This value is very important in fracturing and is usually determined from a minifrac by careful examination of the pressure decline after the pumps have been shut down. It can be estimated by the following **Eq.3:** $P_c = \frac{v}{(1-v)} * [P_{ob} - \alpha_v] + \alpha_h * P_p + \varepsilon_x * E + \sigma_t$ (3) P_c closure pressure [psi] v Poisson's ratio α_v vertical Biot's poroelastic constant α_h horizonal Biot's poroelastic constant P_p pore pressure [psi] ε_x regional horizontal strain, microstrains E Young's Modulus [psi] σ_t regional horizontal tectonic stress [psi]
Extension pressure, P_{ext}	This is the pressure required in the frac fluid in the fracture in order to make the fracture propagate. It is usually 100 to 200 psi greater than the closure pressure, and this pressure differential represents the energy required to actually make the fracture propagate, as opposed to merely keeping it open (i.e. P_c). In hard formations, fracture extension pressure is close to the closure pressure. In softer formations, where significant quantities of energy can be absorbed by plastic deformation at the fracture tip, extension pressure can be significantly higher than closure pressure. The fracture extension pressure can be obtained from a step rate test, which is performed prior to the real hydraulic fracturing treatment as a calibration test. In step rate test an injection fluid is injected for a defined period in a series of increasing pump rates, the resulting pressures are fixed and are used to adjust the fracture model to the actual formation pressure response.
Net pressure, P_{net}	This is the difference between the fluid pressure in the fracture and the closure pressure. P_{net} is a measure of how much work is being

	performed on the formation. By analyzing the trends in P_{net} a great deal can be determined about how the fracture is growing – or shrinking. Net pressure is calculated by **Eq.4**: $$P_{net} = P_{bht} - \Delta P_{nwb} - P_c \qquad (4)$$ P_{net} net pressure [psi] P_{bht} bottomhole treating pressure [psi] P_{nwb} near wellbore pressure [psi] P_c closure pressure [psi]

2.2 Hydraulic fracturing treatment sequence

Hydraulic fracturing treatment sequence is represented in Figure 3. Normally, it consists of three stages. The first stage includes pad fluid injection, which is determined as the fluid that does not contain proppant. The injection continues until the wellbore pressure becomes equal to breakdown pressure, at this point the formation breaks down, the fracture is created and the injected fluid leaks off into formation. Further on, the fracture continues to propagate and to open more formation as the pumping rate is maintained higher than the fluid loss rate.

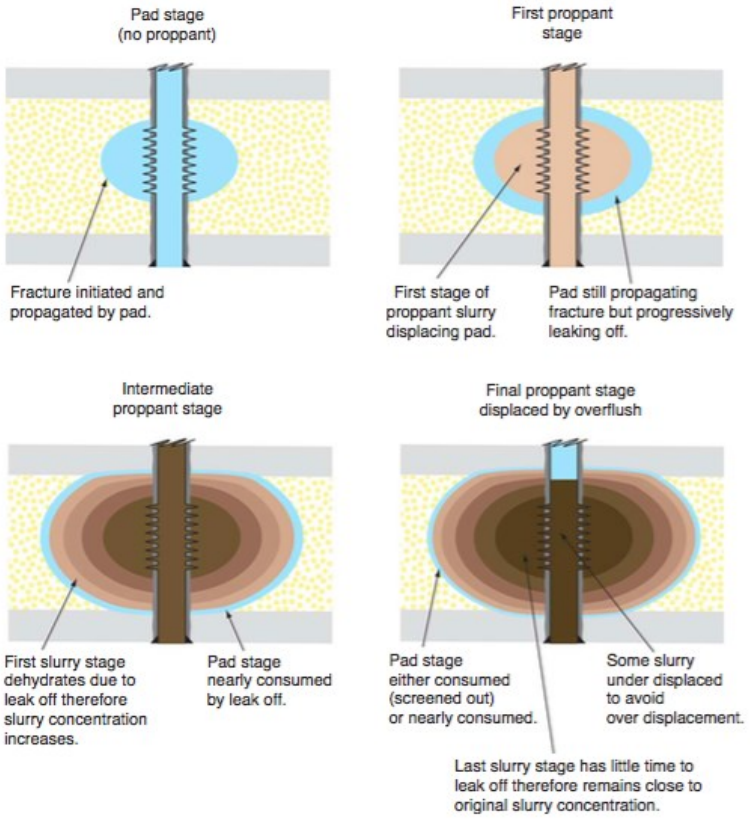

Figure 3: Hydraulic fracturing treatment sequence [2, p. 89]

The second stage consists of injecting a proppant slurry into the fracture in order to prop the fracture open. Once pumping is stopped and the injected fluids flow back from the well, the propping agent remains in place and keeps a conductive channel open for the increased formation flow area during production. The slurry concentration is increased with each stage until the entire fracture is filled with the design concentration slurry.

The final stage includes the flush stage pumping, which is intended to sweep the wellbore clean of proppant. Usually this is performed with just water with friction reducers (slick water), sometimes with additives to prevent hydrates occurring if gas percolates back from the fracture. The well is generally then shut-in for some period to allow fluid to leak off such that the fracture closes and stresses the proppant pack. Shut-in also allows temperature (and chemical breakers added to the fluid while pumping) to reduce viscosity of the fracturing fluid.

The proppants must not be over-displaced, because if over-displaced, the critical near-wellbore area of the fracture will not be propped. Under-displacement may be determined at 10% of the volume less, however, the under-displaced volume of propppant must be removed by coiled tubing prior to production.

Ideally, this process leaves a proppant-filled fracture with a productive fracture length (or half-length), propped fracture height and propped fracture width (which determines the fracture conductivity).

2.3 Pretreatment formation evaluation

Before performing hydraulic fracturing treatment, a lot of considerations should be taken into account, such as geology, petrophysics, well testing data in order to get a completed understanding of the reservoir. The sources of data are represented in Figure 4.

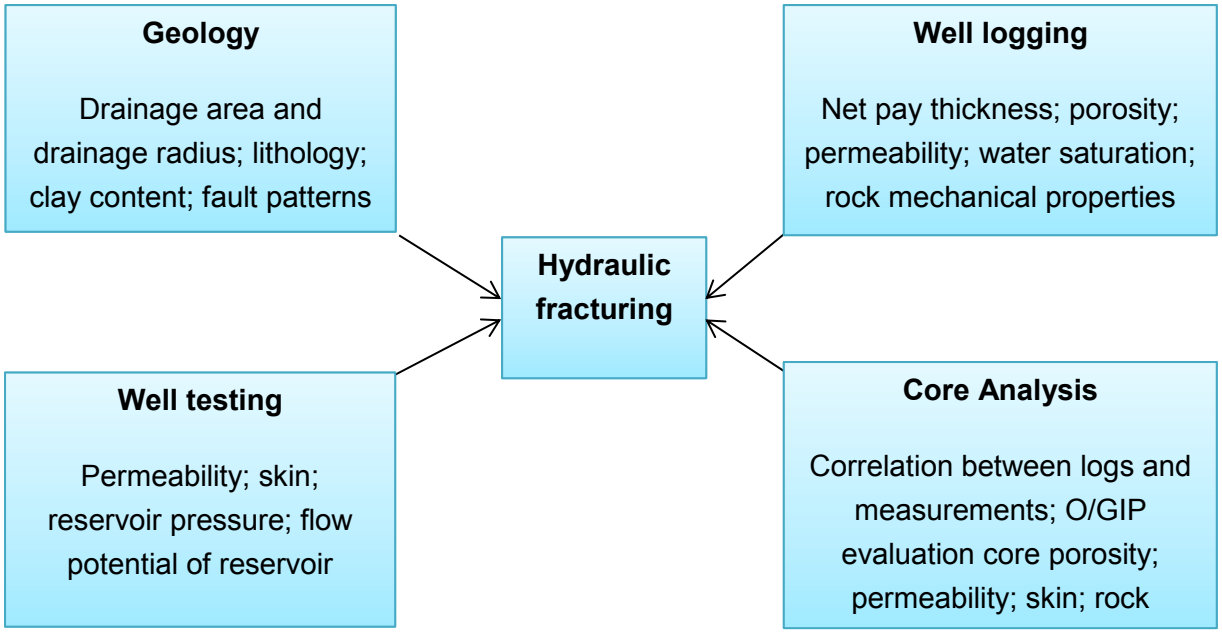

Figure 4: Data sources for hydraulic fracturing treatment

It is vital to understand geologic deposition patterns and drainage area, as the engineer must determine optimum values of fracture lengths and drainage radius. Lithology influences the selection of the hydraulic fracturing fluid. For instance, in sandstone reservoir, a water based or oil based fracturing fluid is selected, whereas in shallow carbonate reservoirs sometimes acid based fluid is feasible. Clay reduces the permeability of the reservoir, therefore, it is important to understand the pore filling and material distribution for the successful job planning. In-situ stresses in rocks may be investigated by analyzing the regional and local fault systems.

Based on the data obtained in logs, the shale content, oil and gas in place, as well as rock mechanical properties may be estimated. The most important mechanical properties include Young's modulus, Poisson's ratio, shear and bulk modulus, compressibility. These properties are required to determine the stress profile, which is crucial to design a fracture treatment.

Conventional core analysis is usually done to calculate the values of porosity, permeability and water saturation at atmospheric conditions. Special core analysis is done under simulated reservoir conditions and is used to identify values of porosity, capillary pressure, relative permeability to oil, gas, water, saturation exponent and cementation factor. In addition, compressional, shear wave time and density might be measured in laboratory. Oriented coring technique is useful to determine the direction of natural and induced fractures and stress patterns.

The main purpose of the well test is to identify the dynamic reservoir permeability, skin factor and initial reservoir pressure, in-situ stresses and effective fluid loss. In order to perform a successful pretreatment evaluation, all available data sources must be used.

2.4 Hydraulic fracturing design

Hydraulic fracturing treatments design is based upon the knowledge obtained from pretreatment formation evaluation to maximize net present values (NPVs) of the fractured wells. Specifications of fracturing fluid and proppant, fluid volume, proppant weight requirements, fluid injection schedule, proppant mixing schedule and predicted injection pressure profile should be planned properly before going to the field operation. A hydraulic fracturing design includes several steps.

1. Selection of the fluid

The major considerations for the fluid selection include viscosity (for width, proppant transport, fluid-loss control) and cleanliness (after flowback) to produce maximum post fracture conductivity. Fracturing fluid controls the efficiencies of carrying proppant and filling in the fracture pad.

2. Selection of a proppant

Major considerations for the proppant selection include compressive strength and the effect of stress on proppant permeability. Generally, bigger proppants yield better permeability,

however, proppant size must be checked against proppant admittance criteria through the perforations and inside the fracture.

3. Calculation of Maximum Treatment Pressure

The maximum treatment pressure is expected to occur when the formation is broken down. The bottom-hole pressure is equal to the formation breakdown pressure and the expected surface pressure can be calculated by **Eq.5** [2, p.6]:

$$P_{si} = P_{bd} - \Delta P_h + \Delta P_f \qquad (5)$$

P_{si} surface injection pressure [psi]
P_{bd} breakdown pressure [psi]
ΔP_h hydrostatic pressure drop [psi]
ΔP_f frictional pressure drop [psi]

4. Selection of Fracture Models

For the selection of the proper model, it is necessary to consider availability and quality of input data. One group of data includes such parameters that can be adjusted by an engineer, such as the well completion details, treatment volume, pad volume, injection rate, fracture fluid viscosity, fracture fluid density, propping agent type and propping agent volume. The second group of data includes the measured or estimated data, that can't be controlled by an engineer. Formation depth, formation permeability, in-situ stresses, formation modulus, reservoir pressure, formation porosity, formation compressibility, and the thickness of the reservoir refers to the second group.

There are three modes of failures that are conventionally defined, as depicted in Figure 5. Mode I fracture is a pure tensile opening. This mode is only recognized and handled by conventional linear-elastic fracture mechanics (LEFM) models. Model II describes shear failure through sliding in the direction on applied load. Mode III fracture is a tearing or lateral, out-of-plane shear mechanism.

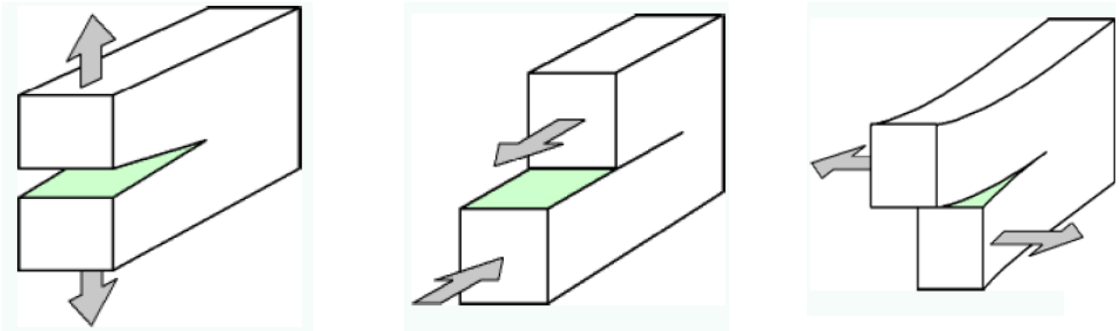

Mode I: Tension Mode II: Sliding shear Mode III:Tearing shear

Figure 5: Modes of failure mechanism [4, p. 6]

The basic fracture geometry characteristics include: height H, half length X_f and width W. Once these three characteristics have been determined, other quantities such as proppant volume, fracture conductivity and ultimately production increase can be determined. It is usually assumed that the two wings of the fracture are identical and 180 º apart (i.e. on opposite sides of the wellbore). This is not necessarily the case. It is also normal to model the fracture wings as being elliptical in shape - however, the reality is that the geometry is probably quite a bit more complex.

All available fracture models may be divided into several categories based on the way they handle the fracture growth. Each model considers a set of specific assumptions, therefore, each of them has particular strengths and weaknesses. The fracture categories are the following:

- 2D models (Perkins-Kern-Nordgren (PKN), Kristianovich and Zheltov - Daneshy (KZD) and radial);

- Pseudo-3D models (MFrac, StimPlan, e-Stimlab, FracCade);

- Lumped parameter models (FracPro, Fracpro-PT);

- 3D Models (GOHFER®, N-Stimlab, Terra-Frac).

The basic 2 D geometries are depicted on Figure 6. In the PKN geometry the ellipse is assumed in the vertical pane. In this model the characteristic length is a total frac height and the width increase with the increasing pressure. PKN models are highly dependent on fluid rheology due to the fact that the increase in pressure in this model is assumed to come from the viscous pressure drop of fluid along the fracture length. In the KZD model, the ellipse is assumed to be in a horizontal plane and the characteristic length is the tip-to-frac length. Therefore, the solution for such model is normally written using the fracture half-length from wellbore to tip. This model assumes a shear failure at target bed boundaries that form the primary height containment mechanism. As the fracture grows in length, the treating pressure drops or the width becomes very large. The KZD model is relatively insensitive to fluid rheology due to the large predicted width, shorter length, and smaller pressure gradient along the fracture length. In the radial model fracture length is the function of the radius or half-length of fracture. This produces a fracture of circular shape.

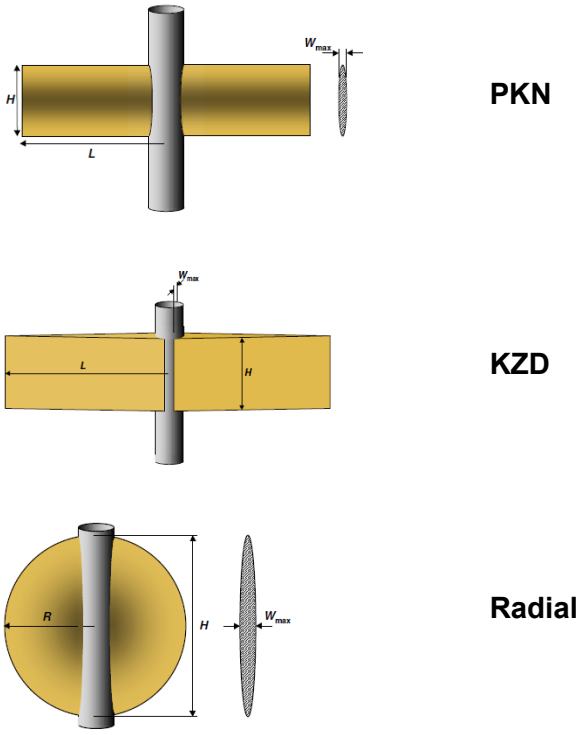

Figure 6: Basic 2D fracture models (W_{max}- maximum width; L-fracture half-length; H-fracture height, R-fracture radius) [3, pp. 68-70]

The Pseudo 3D model the fracture is assumed to be elliptical in cross section along its entire length, and this length is sub-divided into elements. The internal pressure is calculated then for each element and is afterwards used to estimate the height of the fracture in that element. The width profile is calculated using the same equation as the PKN model. The length is estimated from the material balance equation once leakoff is accounted for based on the known height and width. An example of Pseudo-3D fracture model is represented in Figure 7. This model is limited by the assumption of the linear elastic deformation, the elliptical frac shape, stress intensity factor and singularity at the fracture tips, and the assumptions of complete elastic coupling. Such model fails if the fracture can not be described as a continuous entity from upper and lower tip in any element.

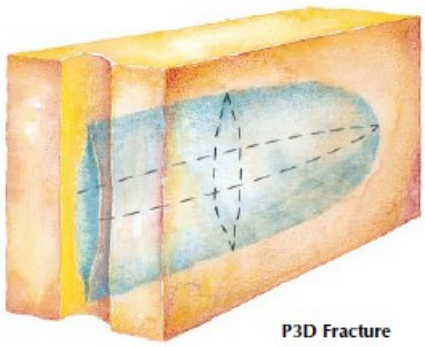

Figure 7: P3D fracture model [5, p. 10]

Lumped parameter models describe the fracture growth only at three points: the points at the upper, lower and lateral tips of the fracture. Therefore, the fracture is assumed to have a ‘’semi similar’’ elliptical shape that is defined by connecting these points. An example of such model is depicted in Figure 8. In this model, the fracture growth is driven by vertical and horizontal pressure gradient functions. The result is a very wide predicted fracture with a relatively short length, caused by user-controlled input functions rather than measured rock properties.

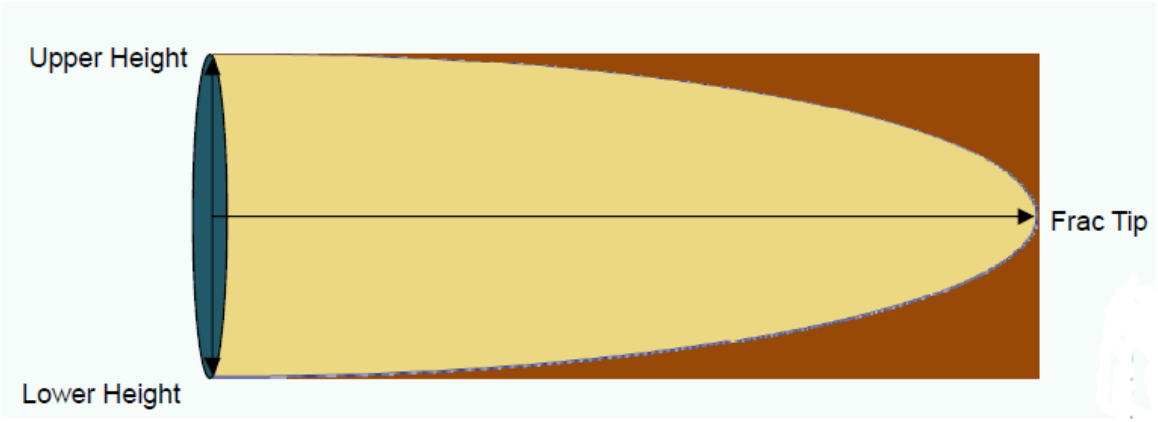

Figure 8: Lumped parameter model [4, p. 19]

There are three models that can be considered as 3D. N-Stimlab is the newest model, which uses the gridded width and flow solution similar to GOHFER®. It relies on a linear-elastic coupling of the rock. The Terra-Frac model relies on a trinangular mesh finite element width solution with fully coupled elastic deformation and stress intensity factir tip conditions. It is limited to a single flid injection point and it requires re-meshing with time.

GOHFER® model uses the gridded deformation solution and attempts to predict the expected discountinuous nature of the rocks with bedding planes, planes of weakness or incipient failure and pre-existing natural fractures and fissures. In addition, it provides a shear-decoupled formulation of fracture, because based on the field results the shear failure and slip commonly occurs during the hydraulic fracturing operation. Therefore, it is considered one of the most reliable fracture simulators. In addition, it contains a big database of the fluid rheology and proppant transport models, that have been extensively tested by laboratory research.

5. Selection of Treatment Size

The optimum design for a conventional fracture treatment is one in which the pad volume has leaked off into the formation and the proppant has reached the tip at the end of pumping, leaving the fracture filled with the proppant-laden slurry to provide a fairly uniform propped width and sufficient conductivity to minimize the pressure drop during production [6, p. 18]. Treatment size is primarily defined by the fracture length. Fluid and proppant volumes are controlled by fracture length, injection rate, and leak-off properties. A general statement can be made that the greater the propped fracture length and greater the proppant volume, the

greater the production rate of the fractured well. Limiting effects are imposed by technical and economic factors such as available pumping rate and costs of fluid and proppant. Within these constraints, the optimum scale of treatment should be ideally determined based on the maximum net present value (NPV).

6. Production forecast and NPV Analyses

The hydraulic fracturing design is finalized on the basis of production forecast and NPV analyses. The information of the selected fracture half-length X_f and the calculated fracture width w, together with formation permeability (k) and fracture permeability (k_f) can be used to predict the dimensionless fracture conductivity F_{CD} with **Eq. 6**:

$$F_{CD} = \frac{k_f \times w}{k \times x_f} \qquad (6)$$

F_{CD} dimensionless fracture conductivity
k_f fracture permeability [mD]
w fracture width [ft]
k formation permeability [mD]
x_f fracture half-length [ft]

Comparison of the production forecast for the fractured well and the predicted production decline for the unstimulated well allows for calculations of the annual incremental cumulative production for a well with **Eq.7**:

$$\Delta N_{p.n.} = N_{p.n}^{f} - N_{p.n}^{nf} \qquad (7)$$

$\Delta N_{p.n.}$ predicted annual incremental cumulative production for year n [ft^3]
$N_{p.n}^{f}$ forecasted annual incremental cumulative production of fractured well for year n [ft^3]
$N_{p.n}^{nf}$ forecasted annual incremental cumulative production of non-fractured well for year n [ft^3]

Based on the results, the incremental revenue, net present value of fracturing project may be estimated.

2.5 GOHFER 3D geometry fracture simulator

Different numerical simulators are used nowadays to evaluate and predict the location, direction and extend of the hydraulic fractures. Simulations range from two to fully three dimensional depending on the degree of complexity of the wellbore and fracture geometries, the required accuracy of predictions.

The three main fracture simulation models used in the industry today are FracPro, FracproPT and MFrac. They are used in 90% of all treatments currently performed. Other simulators, such as StimPlan, GOHFER® and the proprietary simulators produced by Schlumberger,

Halliburton, Shell and others, are available, but their use is limited mainly to engineers who work for the actual company that produced the simulator [3, p. 91].

GOHFER® 9.0.0.120 license was used in the current work. With the help of this simulator the hydraulic fracturing treatment was modelled, the fracture geometry and post treatment production profile were analyzed.

GOHFER®, which stands for Grid Oriented Hydraulic Fracture Extension Replicator, is a planar 3-D geometry fracture simulator with a fully coupled fluid/solid transport simulator.

The model takes a finite element approach to fracture propagation, modelling the reservoir and the formations above and below it as a series of elements, rather than as a continuum. The fracture propagates along a plane between elements, so in order to produce fracture width, elements either side of the fracture have to be compressed. At the fracture tip, there is a single element just ahead of the fracture, so that the tip is positioned at some point on the side of the element. Fracture propagation occurs when the tensile stress in the element exceeds the failure criterion for the material, and the element splits into two pieces, along the plane of the fracture. The fracture has then propagated by a distance equal to the width of the element.

The advantages of this approach are that it is very simple to give each element its own set of rock mechanical and reservoir properties, making simulation of multiple formations very easy. In addition, most available models today are assumed to be linear elastic, which means that the fracture walls are coupled together, which results in elliptical shaped fractures and more height growth. However, the rocks are not linear elastic. For this reason, GOHFER® uses a shear decoupled 3D model, which means that the rocks are allowed to fail in shearing at the bedding planes and discontinuities.

The benefits of the software also include [7, p. 2]:

- Possibility to directly import digital log data and to create a lithological description. The in-situ stress profile is internally calculated from pore pressure, poroelasticity, elastic moduli and geologically consistent boundary conditions;
- Horizontal and asymmetric facture modelling, including complex reservoir geometry;
- Vertical and horizontal anisotropy is taken into account;
- Multiple perforated intervals can be designed (limited entry design, modelling of multiple fracture initiation sites simultaneously, modelling of perforation erosion).

Software capabilities include:

- Pressure diagnostics analysis based on the available data from step-rate, falloff and after closure analysis;
- 3D fracture geometry simulation;
- Production forecast and NPV calculations.

3 Fracturing fluids and proppant agents

This chapter describes in detail the fracturing fluids and propping agents that are available at the market today. In particular, it considers the required properties of the fracturing fluids, their composition, additives and application areas, as well as physical properties of proppants and the selection criteria.

3.1 Properties of fracturing fluids

There is a list of specific chemical and physical properties, that fracturing fluid must fulfill [8, p. 29]:

- Compatibility with formation material and fluids;
- Capability to develop the necessary fracture width to accept proppants;
- Sufficient viscosity to transport proppant: yield viscosity quickly and maintain viscosity at shear and temperature;
- Low (or controlled) fluid loss- the special fluid loss additives, such as microemulsions, bridging and plastering agents are used for this purpose;
- Low friction in pipe;
- Clean breaking: break after desired temperature; break to low viscosity and no yield-point;
- Non-damaging: no residue is left behind; do not cause capillary or phase trapping;
- Simplicity of the fluid preparation in the field;
- Cost-effectiveness-fracturing fluid efficiency must be proved by economic analysis prior to execution.

3.2 Types of Fracturing Fluids

The optimal selection of the hydraulic fracturing chemical composition depends on the type of reservoir. The fracturing fluids may be classified into the following groups:

- Water-based fluids;
- Oil-based fluids;
- Foam fluids;
- Acid fluids.

Water-based fluids are the most widely used fracturing fluid due to the list of advantages they have in comparison with other fluid, such as low cost; availability due to a greater variety of chemical compounds that are more soluble in water than in oil; easiness to viscosify and to control; incombustible properties; increased hydrostatic head yield.

Oil-based fracturing fluid have currently a limited use. However, they are applied in water sensitive oil-producing formations that have a tendency to swell in contact with water.

The main disadvantages of oil-based fluids are:

- Fire hazard;
- Higher friction losses;
- Higher pumping pressures requirements;
- The temperature stability of oil-based fluid is less predictable than a delayed, cross linked water-based fluid,
- Complicated fluid preparation and high requirements for quality control:
- Very expensive in comparison with water base.

Foam represents the mixture of oil and gas, stabilized with surfactants. They help to stabilize the thin liquid films and prevent cells from coalescing. Foams are prepared by introducing either nitrogen or carbon dioxide to the liquid mixture. However, due to the higher solubility in water and oil, more material (nitrogen or carbon dioxide) is needed to saturate water and to create a foam, leading to increased material costs.

Acid fluids are used in the acid fracturing operations. The most commonly used acid fracturing fluid is HCl. The main difference between acid fracturing and proppant fracturing is the way fracture conductivity is created. In comparison to normal proppant fracturing, where the fracture is propped open after the treatment completion with the help of the propping agent, in acid fracturing, the acid is used on order to “etch” channels in the rocks, thus creating the walls of the fracture. Acid fracturing is mostly used in for low-permeability, acid-soluble rocks, such as carbonate reservoirs and should never be used for sandstone, shale or coal-seam reservoirs stimulation.

The more detailed description of water-based fluid types is reflected in Table 2.

Table 2: Water based fluid types [8, pp. 17-21]

Base fluid	Fluid type	Description
Water based fluids	Linear	These are the fluids without chemical cross linked structures. Despite its simplicity in terms of control and application, the main disadvantages of linear fluid are a poor proppant suspension capability and less temperature stability in comparison with a similar cross linked fluid. Therefore, its application is limited to low temperature conditions and short fractures design. For a deeper penetration of proppant, the more viscous cross linked fracturing fluid is a preferred option.
	Cross linked	Benefits of these fluids include: higher viscosity in the fracture with a comparable gel loading; higher efficiency in fluid loss control; improved proppant-transport capabilities; better temperature stability. However, regardless of the gel composition or viscosity, all fracturing gels tends to thin with shear rate and heat. Hence, as a result very high

		shear rates may lead to irreversible loss of the viscosity of the cross linking fluid. Due to this fact, the use of 'standard' cross linked gel systems has declined and have been replaced by delayed cross linked fracture-fluid systems.
	Delayed Cross linked	In this system the crosslink time is controlled. The crosslinking rate may be controlled by different parameters, such as fluid temperature, shear conditions, cross linker type and the presence of organic compounds that react with the cross linker. For instance, slow dissolving of cross linkers can also be used to delay crosslinking. The main advantages of a delayed cross linked system include: better dispersion of cross linker; better long-term stability at elevated temperatures; lower friction pressures which allow higher injection rates and lower horsepower requirements.

3.3 Fracturing fluids additives

The main fracturing fluids additives are depicted in Table 3.

Table 3: Fracturing fluid additives [8, pp. 35-202]

Fluid additive name	Function	Materials
Gelling additive	Increase the viscosity, which leads to increase of the fracture width, reduction of the fluid loss, improvement of fluid efficiency and proppant transport, as well as the friction pressure reduction.	Guar polymer Hydroxypropyl guar (HPG) Carboxymethyl HPG (CMHPG) Hydroxyethylcellulose (HEC) Hydropropylcellulose (HPC) Xanthan gum Polyacrylamides
Cross linkers	To increase the base viscosity of the linear gel, elasticity and proppant transport capability of the fluid.	Borate ions, aluminum, copper, manganese, chromium, titanium chelates, and zirconium chelates.
Fluid loss additives	To form a filter cake and therefore to reduce leak off in	Guar gum, silica flour, diesel fuel, calcium carbonates and

	formation.	lignosulfonate, natural starch, oil soluble resin.
Breakers	To enable a viscous fracturing fluid to be degraded controllably to a thin fluid that can be produced back out of the fracture. This is done in order to increase the permeability of the proppant pack to oil and gas and therefore, enhance the effectiveness of the treatment.	Oxidizers and enzymes.
Bactericides	To prevent viscosity loss caused by bacterial degradation of polymer.	Glutaraldehyde, chlorophenates, quaternary amines and isothiazoline.
Clay stabilizers	To prevent clay disintegration, which may lead to narrow pores bridging and permeability reduction.	Potassium chloride, ammonium chloride, calcium chloride and polymeric clay stabilizers.
Surfactants	To reduce the surface tension of the fracturing fluid to improve fluid recovery and compatibility between the fracturing fluid and the formation matrix or formation fluids.	
Buffers (pH Control Additives)	To adjust and maintain the pH of the base fluid.	Ammonium, potassium, sodium bicarbonate, fumaric acid, soda ash or combination of these materials.
Friction reducers	To reduce the friction as the fluid is pumped down the well tubulars, hence, to reduce drag in tubings.	Low concentration of polymers and copolymers of acrylamide are the most efficient and cost-effective friction reducers used for fracturing fluids.

3.4 Proppants

Proppants are special propping agents that are used to hold the fracture open after the pumping pressure is no longer subject to the well and the fracturing fluid has leaked off. Hence, their main function is to provide and maintain conductive fractures during well production.

The fracture conductivity is a measurement of how a propped fracture is able to convey the produced fluids over the producing life of the well. It is affected by many factors, such as proppant composition, its physical properties, proppant-pack permeability, movement of formation fines in the fractures, long-term degradation of the proppant [9, p.27].

3.4.1 Physical properties of proppants

The following physical properties influence the fracture conductivity:

- grain size and grain-size distribution;
- roundness and sphericity;
- proppant density;
- proppant strength;
- quantities of fines and impurities.

Grain size and grain-size distribution. The proppant grain size and grain size distribution are two important parameters for hydraulic fracturing treatment. Proppant sizes are generally between 8 and 140 mesh (105 μm - 2.38 mm). Mesh size is the number of openings across one linear inch of screen. Proppant sizes are often descried as sieve cut. For example, 16/30 mesh is 595 μm -1190 mm; 20/ 40 mesh is 420 μm - 841 mm; 30/50 mesh is 297 μm -595 mm; 40/ 70 mesh is 210 μm - 420 mm; 70/140 mesh is 105 μm -210 mm [9, p.27].

Generally, higher fracture conductivity is given by the larger proppant particle size. Therefore, in the traditional fracture treatment the smaller particle size proppants are introduced to the well first and afterwards larger particle size proppants are tailored to maximize the near wellbore conductivity.

Roundness and sphericity. Proppant grain roundness is a measure of the relative sharpness of the grain corners, or grain curvature. Particle sphericity is a measure of how close the proppant particle or grain approaches the shape of a sphere. Ideally, proppant shape should be spherical and non-angular because in this case, stresses are more evenly distributed on the proppants and a tighter proppant pack is reached. Angular grains have a tendency to fail at lower closure stresses, which leads to fines production and permeability reduction.

Proppant density. Proppant settling rate increases linearly with the density. It is more difficult to suspend high-density proppants in the fracturing fluids, as well as to provide efficient transport to the fracture top. Settling reduction may be compensated by using high-

viscosity fluids or by increased injection rate in order to reduce the required suspension time. In addition, more high-density material is required to fill a given fracture volume.

Proppant strength. If the proppant strength is inadequate, then proppants can be crushed by the clossure stress and produce fines, which contribute to the lower permeability and proppant pack conductivity reduction.

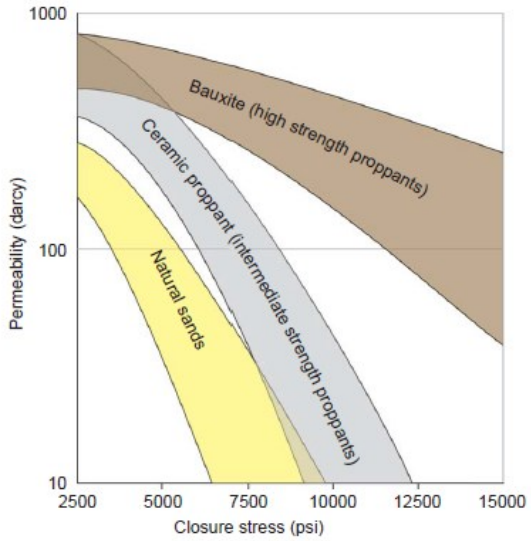

Figure 9: Strength comparison of various types of proppants [2, p.92]

Figure 9 represents the strength comparison of proppants. From the figure it may be concluded, that different types of proppants may be characterized by the following closure stresses ranges:

- sand- up to 6000 psi;
- resin-coated proppant- up to 8000 psi;
- intermediate- strength proppant (ISP)- from 5000 psi up to 10000 psi;
- high-strength proppant- closure stresses at or greater than 10000 psi.

Proppant type and size should be determined by comparing economic benefits versus cost.

Figure 10 shows the stress at which conductivity of 1750 mD*ft is maintained for different types of proppants. This confirms that higher density materials can withstand higher stress in order to maintain the same conductivity.

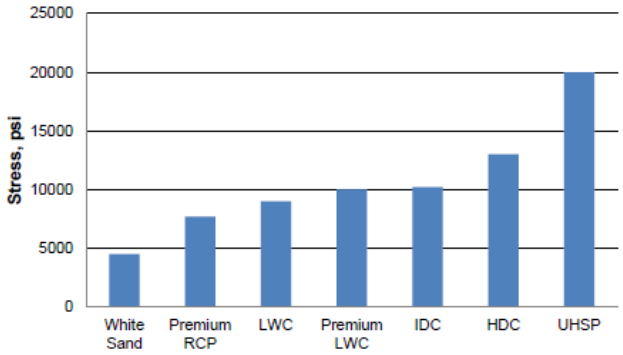

Figure 10: Stress at which conductivity of 1750 mD*ft is maintained [9, p.31]

3.4.2 Basic types of proppants

Basic types of proppants are depicted in Table 4.

Table 4: Basic proppant types [2]

Proppant type	**Description**
'Frac sand' or 'silica sand'	The most commonly utilized due to economic advantages. It is composed of processed and graded high-silica content quartz sand. Two major types of frac sand are so-called white sand and brown sand. Brown sand has a higher impurity content than white sand, which is why it is more prone to crushing at lower stresses. Brown sand is cheaper than white sand.
Ceramic proppants	They are manufactured from sintered bauxite, kaolin, magnesium silicate, or blends of bauxite and kaolin. The main advantages of ceramic proppants in comparison with silica sand are higher strength and higher crush resistance, more uniform size and shape, higher sphericity and roundness to yield higher porosity and permeability of the proppant bed. Moreover, they are distinguished by the highest chemical and thermal stability. These properties lead to higher conductivity inside a fracture both in short and long term. From the economical point of view, ceramic proppants are more expensive than uncoated or resin coated sand. Based on the density, ceramic proppants are classified into three groups: lightweight ceramics (LWC), intermediate density ceramics (IDC), high density ceramics (HDC) and ultra-high strength proppants (UHSP). The proppant density and strength is correlated with the alumina content.

Resin coated proppants (RCP)	Resin systems are commonly made from reactive polymer and a curing agent/hardener. This coating is applied to sand, glass beads and ceramic proppants as well. Resin coating creates a trap for the pieces of broken grain within the coating, thereby it prevents proppant flowback to wellbore. One of the applications also includes prevention of sand production in soft formations. The main disadvantage of this technology is low softening temperatures or low degradation temperatures due to the fact that resin is produced on the basis of polymers.
Ultra-lightweight proppants	They help to reduce proppant settling, improve distribution in the fracture and in combination with the low fluid viscosity application contribute to the increased propped length. The lightweight proppants are the preferred option in shale reservoirs. This is due to the fact, that they can be efficiently carried by the low viscosity slick water, that is generally used as the fracturing fluid in this type of formation, whereas high density proppants can’t.

4 BEER® Fluid

In chapter 4 the BEER® technology is described. The major outcome of this chapter is the laboratory derived properties of the fluid and glass beads. The fluid preparation, its rheology evaluation, determination of viscosity behavior versus time are the main areas of considerations.

4.1 Technology description

BEER® Fluid stands for the Bio-Enhanced Energy Recovery Fluid. The technology has been proposed, developed and patented by Montanuniversitaet Leoben, Austria. The distinguishing features of the proposed technology are the following:
- it consists only of environmentally compatible components;
- it requires only 4 components instead of 11, which is the usual case for the conventional fluids.

Table 5: Comparison of the conventional fracturing fluid and BEER® fluid [10, pp.6-8]

Chemical components	**Conventional fracturing fluid**	**BEER® fluid**
Water	V	V
Polymers	V	V
Crosslinker	V	
pH control	V	
Gel breaker	V	
Surfactants	V	
Clay control	V	V
Biocides	V	
Conductivity enhancers	V	
Fluid loss additives	V	
Proppants	V	V

In Table 6 the more detailed chemical composition of the BEER® fluid is depicted.

Table 6: BEER® fracturing fluid composition

Chemical Component	**Chemical Mechanism**	**Functional Group**
Water (H_2O)	Main Component	Basis of hydraulic fracturing fluid
Potassium Carbonate	Adjusts the pH of fluid to maintain the effectiveness of other components	Weighting agent, corrosion inhibitor, clay stabilizer, sour gas buffer, friction reducer
Xanthan Gum (polysaccharide)	Thickens the water in order to suspend the sand, increase the viscosity of the fluid	Gelling Agent, Fluid loss control and carrying capacity
Glass Beads	Hold the fractures open when the pressure is no longer being subject to the well	Proppant

Figure 11 depicts the BEER® fracturing fluid.

Figure 11: BEER® fracturing fluid without glass beads (on the left) and with glass beads (on the right)

The main advantages of the BEER® fracturing fluid are described below [10, p.8]:

- Enviromentally fully compatible;
- Legal approval for existing additives;
- Meets technical requirements;
- High flexibility in density (up to 2.6 kg/l);
- Recyclable;
- Transparent setup;
- Cost effective.

The glass beads can be defined as rigid, spherical bodies, designed as a propping agent for hydraulic fracturing. They are made of recycled soda-lime glass that was formed to beads. The chemical composition of these glass beads is Si_2O_3 (min. 65%), CaO (min. 8%), Na_2O (min. 14%), Al_2O_3(0.5-2.0%), Fe_2O_3 (max. 0.15%), MgO (min. 2.5%), and others (max. 2%). The specifications are represented in Table 7.

Table 7: Glass beads specifications [11]

Property	**Specifications**
Specific gravity	2.45 to 2.50 g/cm ^{3}
Bulk weight	1.5 kg/l
Hardness (Mohs)	5.5
Toxicity	None
Color	Clear/ Colorless
Configuration	Spherical
Roundness	65 to 95%
Size ranges	425-850 μm; 850-1000 μm

The size range of glass beads represented in Table 7 are those considered for the hydraulic fracturing simulation performed in this work.

Glass beads are represented in Figure 12.

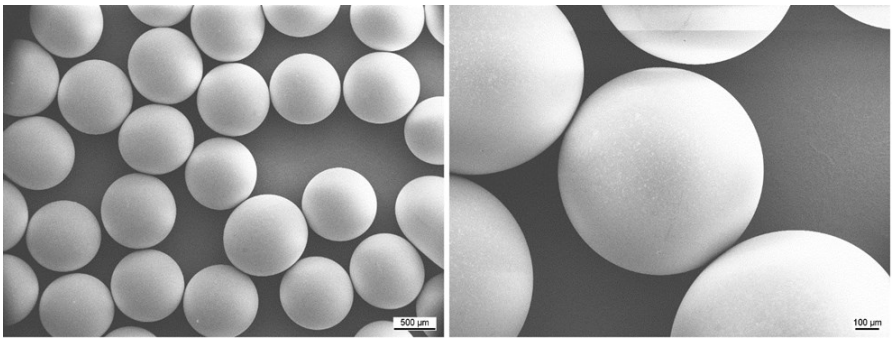

Figure 12: Glass beads under scanning electron microscope [10]

The main advantage of glass beads in comparison with other types of proppants is roundness, which is considered to contribute to the more even packing of the proppants and better permeability.

4.2 Fracturing fluid rheology

Fracturing fluids are complex, non-Newtonian fluids. Their properties are extremely sensitive to shear rate, temperature, minor additive concentrations, proppant types, mix water chemistry, age of chemicals, and many other factors. It is difficult to quantify these properties, however, characterizing these properties and understanding impact of rheology plays an important role for the treatment success.

Most of the service companies use a Power law rheology model to characterize hydraulic fracturing fluid. The model assumes that the fluid viscosity changes as the function of the local shear rate. It describes the typically seen ‘”shear thinning” behavior, in which viscosity decreases at increased shear rates. The apparent viscosity can be calculated by the **Eq.8** below. The large conversion factor 47879 is used in order to convert viscosity to oil field units, cP.

$$\mu_{app} = 47879 \times k' \times \gamma^{\,n'-1} \qquad (8)$$

k‘ fluid consistency index [lb*s^n‘/ft^2]

γ shear rate [1/s]

n’ power law exponent

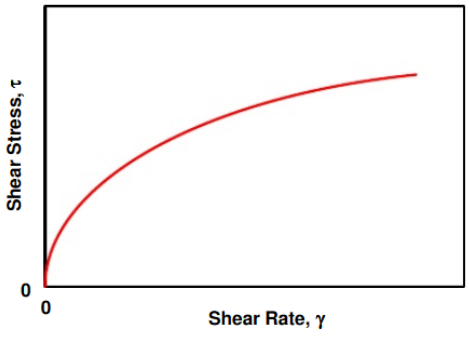

Figure 13: Relationship between shear rate and shear stress for a power law fluid [3, p.21]

The equation above predicts that a plot of viscosity versus shear rate (on a log-log plot) is a straight line. The slope of the line is defined by the rheology exponent n' and the magnitude of the viscosity at particular shear rate is defined by the fluid consistency index k'.

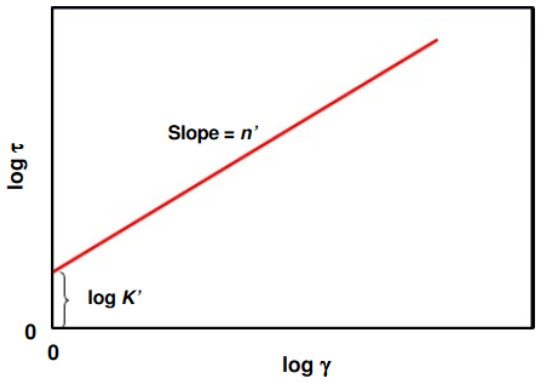

Figure 14: Power law fluid log-log plot [3, p.22]

Power law fluids can be divided into three groups:

- Shear-thinning fluids: in these fluids, n' is less than 1, so that the fluids experience a decrease in apparent viscosity as the shear rate increases. Most of the fluids used for fracturing fall within this category.
- Newtonian fluids: these fluids are a special case of power law fluids in which n' is equal to one, i.e. the viscosity is constant and equal to K'.
- Shear-thickening fluids: these fluids have an n' greater than one, and so exhibit an increase in apparent viscosity as shear rate increases. Extreme examples of these fluids can behave as if they were solids when exposed to even moderate shear force.

Overall, the fluid needs to be optimized to keep outstanding properties of its components, such as friction reduction, corrosion inhibition or clay stabilization, compatibility with rocks, viscosity and also be an economically and logistically friendly product. In order to evaluate all these parameters, lab tests must be conducted.
Based on the available equipment in the university laboratories, such parameters as viscosity versus shear behavior, viscosity versus time behavior, power law exponent and fluid consistency index, fluid density were evaluated and are described in the paragraph below.

4.3 Laboratory tests

4.3.1 Set up

In order to measure the evaluation parameters of the fracturing fluid and glass beads proppants described above, the tests were conducted in the laboratory facilities of the Montanuniversitaet Leoben. The workflow and the main results of the tests are depicted below. The following recipe of the fluids and proportions were proposed by the Chair of Petroleum and Geothermal energy recovery and, therefore, used for the laboratory investigation.

Equipment: graduated flask, electronic scales, mixing device, viscometer, balance scales, magnetic stirrer with heating.
Chemical components: water, xanthan gum (XCD), potassium carbonate (K_2CO_3)

Description: a series of tests were carried out for hydraulic fracturing fluid alone and for the mixture of hydraulic fracturing fluid with the glass beads inside.

The viscosity versus shear rate behavior was analyzed by OFITE Model 800 Viscometer. Furthermore, the density of the fluid was obtained with the help of balance scales.

Table 8: BEER® fracturing fluid recipe [10]

Component	Proportion
Water as a base fluid	1 l
Modified Starch -Xantham Gum	5 g/l H_2O (test №1); 10 g/l H_2O (test №2)
Potassium Carbonate (K_2CO_3)	850 g/l H_2O
Glass Beads	1500g/l H_2O

4.3.2 Fluid mixing and preparation

1. Xanthan gum was poured slowly into the water. It was mixed for 5 minutes, until the components went into solution.

Figure 15: Xanthan gum sample

Figure 16: H_2O with xanthan gum mixture

2. In the next step, K_2CO_3 was accurately added to the mixture and also mixed for 5-7 minutes.

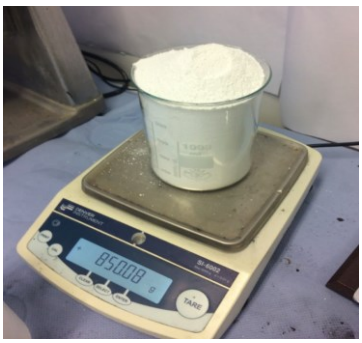

Figure 17: Potassium carbonate

Figure 18: H_2O, xanthan gum and potassium carbonate mixture

3. Finally, very fine glass beads were poured into the fluid and mixed.

Figure 19:Glass beads

Figure 20: Final product

Test №1

It was conducted with the Xanthan Gum concentration of 5 g/l H_2O. The components did not go to the full solution, the phases went into separation. As part of the troubleshooting, the following steps were done:
- Longer mixing period of the fluid components (15 minutes);
- Increasing the concentration of the xanthan gum up to 10 g/l H_2O;
- Adding polypac ultralight component to enhance the rheology of the fluid.

These did not lead to the positive results, therefore, another test was made.

Test №2

The second test was carried out on the basis of the hot tap water. The xanthan gum concentration this time was increased up to 10 g/l H_2O. The results were positive, the components went into solution and no phase separation was observed.

Results

One of the reasons due to which the components did not go to solution in the first test could be the water temperature. In the first test the cold tap water was used, whereas in the second the hot tap water was used. A good practice would be to check for the water temperature and composition, as well as ambient conditions to obtain expected results. Another possible reason could be in the sequence of mixing. In the first test the water was blended with polymer first and then potassium carbonate was added. Based on the obtained results, it is recommended to first blend the water with K_2CO_3 and then add the polymer, as the BEER® fluid might hydrate fast vice versa.

4.3.3 Measuring viscosity

The OFITE Model 800 Viscometer determines the fluid flow characteristics of oils and drilling fluids with relation to shear rate and shear stress over various time and temperature ranges at atmospheric pressure. Speed is controlled with the control knob, shear stress values are displayed on the magnified dial [12].

Figure 21: 8-Speed Viscometer (model 800) by OFITE

Available speeds (shear rates in RPM) are as follows: 3 (Gel), 6, 30, 60, 100, 200, 300, and 600. The Model 800 is suitable for both field and laboratory use and uses a motor-driven electronic package to provide drilling fluid engineers with an extremely accurate and versatile tool.

The Rotor-bob setup used for the measurement is R1B1 type, Torsion spring assemble is F1.0 (Blue).

After the sample had been well mixed, it was proceeded with the viscosity measurement experiments as per the API procedure:

1. The sample was mixed on the “STIR” setting for 10 seconds. The temperature was monitored with a thermometer, 45^0C was fixed.
2. The knob was rotated to one of the speed settings. The reading and the temperature were recorded once the reading stabilized. This step was repeated for other speeds as well.

It must be noted, that the test must always be started with the higher RPM and worked down to the lowest RPM. Therefore, the test was started at 600 RPM, then the speed was reduced correspondingly to 300 RPM, 200 RPM, 100 RPM, 6 RPM and 3 RPM.

Table 9: Xantham gum+water+potassium carbonate (t=45^0 C)

Speed, RPM	600	300	200	100	60	30	6	3	PV	YP
Shear stress, lb/100ft^2	122	84	71	54	45	36	22	19	38	16

Table 10: Xantham gum+water+potassium carbonate+glass beads (t=45 ^{0}C)

Speed, RPM	600	300	200	100	60	30	6	3	PV	YP
Shear stress, lb/100ft^2	180	130	110	83	70	55	36	31	50	26

The results of the laboratory tests are represented in Figure 22.

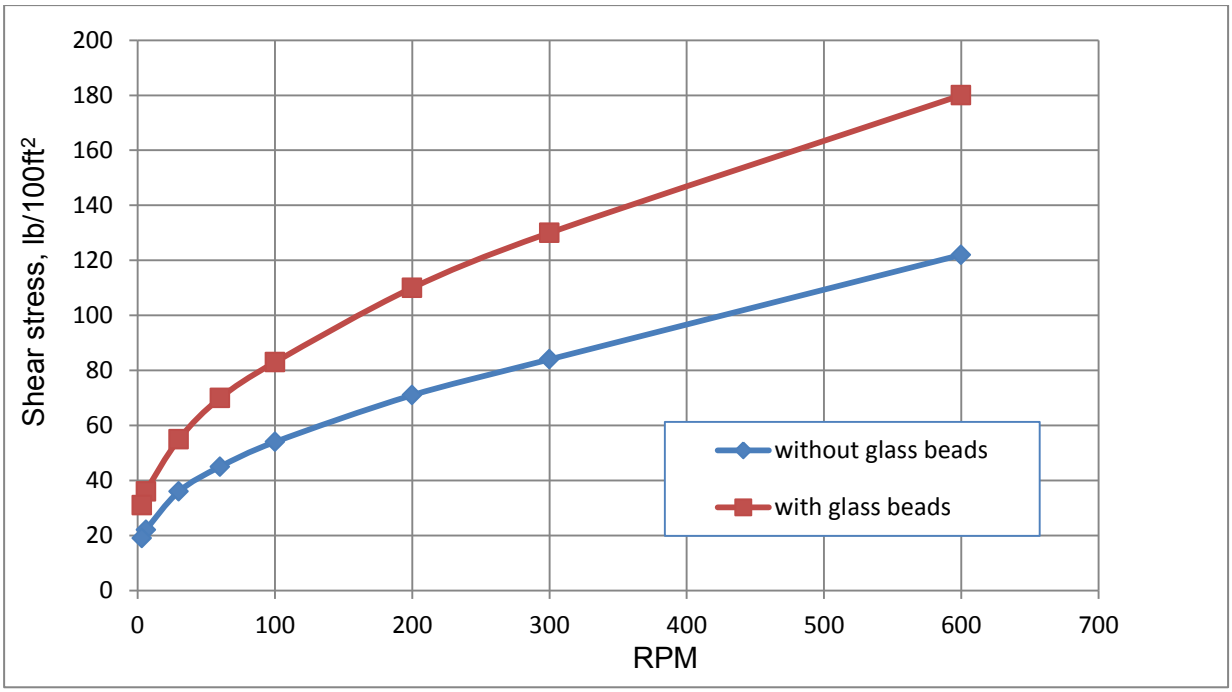

Figure 22: Shear stress versus RPM

Curve shows a nonlinear relationship between the shear rate and the shear stress with a nonzero shear stress value at zero shear rate. An initial force is required to deform and mobilize the fluid. The flow resistance increases less than linearly with deformation. The behavior of this fluid indicates that this is a Herschel- Bulkley fluid.

The flow behavior of such fluids is described by their model and is expressed in **Eq.9**:

$$\tau = \tau_\gamma + K * \dot{\gamma}^n \qquad (9)$$

τ_y yield stress [lb/100 ft^2]

K fluid consistency index [lb/100 ft^2]

$\dot{\gamma}$ shear rate [RPM]

n power law index

The approximate yield stress τ_y, commonly known as the low-shear-rate yield point, should be determined by **Eq.10:**

$$\tau_y = 2 * \theta_3 - \theta_6 \qquad (10)$$

τ_y yield stress [lb/100 ft^2]

θ_3 dial reading at 3 RPM [lb/100 ft^2]

θ_6 dial readings at 6 RPM [lb/100 ft^2]

At high shear stresses it is allowed to treat Hershel-Bulkley fluid as the power law fluid. In this case the assumption that the log-log slope of the Hershel-Bulkley flow equation is quite close to that of Power law equation [13, p.26]. Therefore, the power law index and fluid consistency indexes were determined graphically, as explained in Figure 14.

4.3.4 Measuring the weight

The balance scales were used to measure the weight of the fluid sample. The hydraulic fracturing fluid density without glass beads was determined to be 1,45 kg/l; with glass beads – 1,8 kg/l.

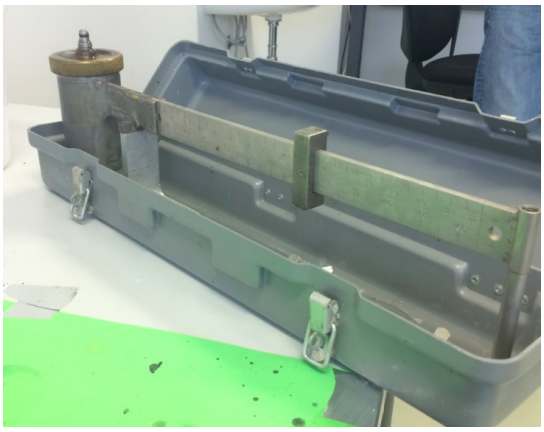

Figure 23: Balance scales measurements

4.3.5 Sweeping frequency tests

Frequency sweep is defined as an oscillatory test with variable frequency and constant amplitude values. In this test, the time-dependent shear behavior is examined. This test was used in order to determine the variable power law fluid and fluid consistency index parameters versus time.

In order to obtain the rheology corresponding to the downhole wellbore conditions considered for further simulation, it has been decided to heat the fluid up to 70^0C. For that purpose the magnetic stirrer with heating was used.

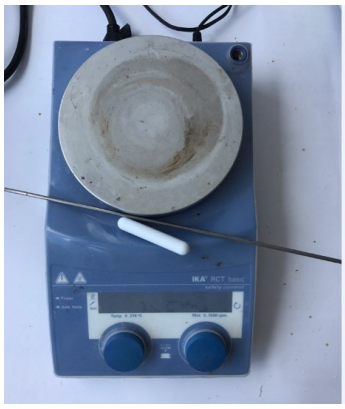

Figure 24: Magnetic stirrer with heating IKA® RCT basic

The series of sweeps have been performed at approximately 5 minutes time interval each and the corresponding shear stresses were fixed. The speed was adjusted from 600 to 3 RPM and the values for the shear stress were obtained. The duration of the overall test was 65 minutes. As an example, Figure 25 illustrates the shear stress versus shear rate behavior of the fluid after 35 minutes of tests.

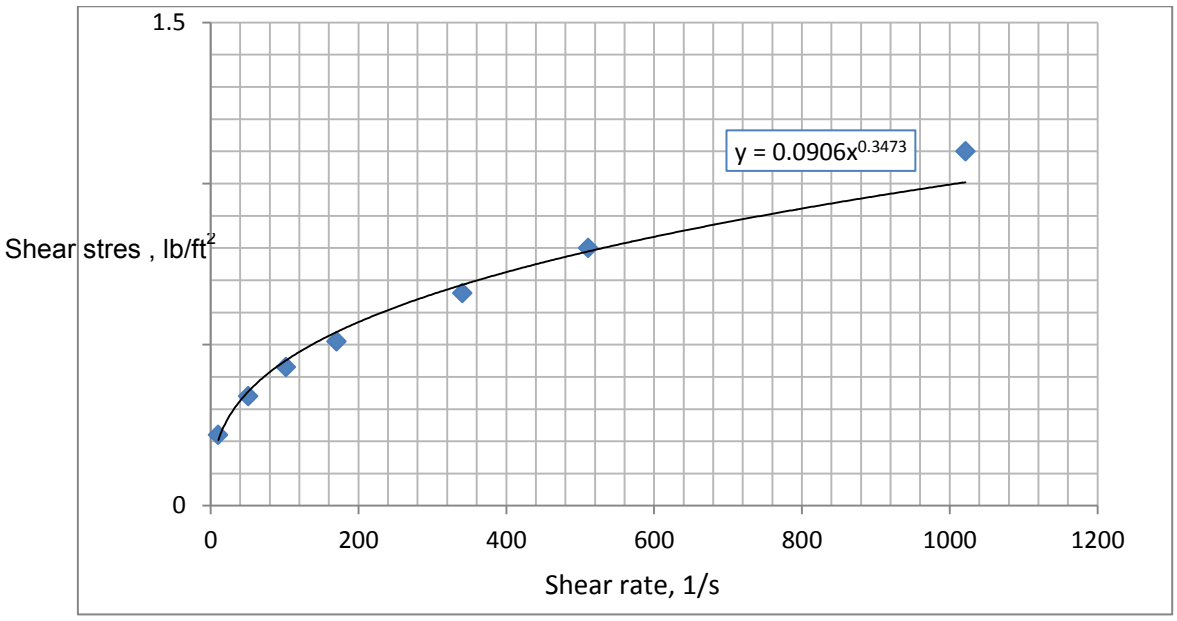

Figure 25: Shear stress versus shear rate fluid behavior (t=70^{0}C, t=35 min)

In order determine n‘ and K‘, the shear rate and shear stress were plotted on a log-log scale. After that in Microsoft Excel 2010, the power law trend was applied and n‘ and K‘ values were estimated. Figure 26 illustrates the log-log plot of shear stress versus shear rate.

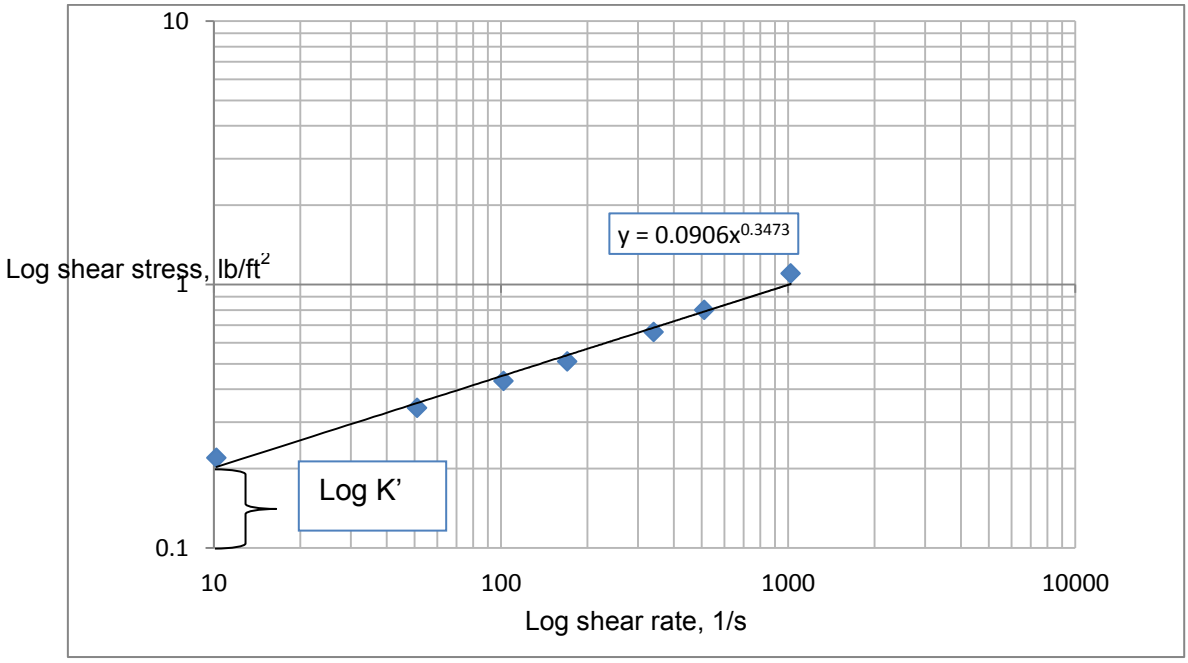

Figure 26: Log-log plot of shear stress versus shear rate (t=70^{0}C, t=35 min)

In this example, K'=0,0906 lb*s^n'/ft^2, whereas n'=0,3473. These graphs have been made for each time step and corresponding values of K' and n' were graphically obtained. After that, the viscosity as a function of n‘ and K‘ was calculated at the shear rate of 170 sec^{-1} by the **Eq.8** in Subchapter 4.2. The results of the calculation are represented in Table 11.

Table 11: Viscosity, power law and consistency fluid index versus time

Time, min	n‘	K‘, lb*s^n‘/ft^2	μ_{eff}, cP
5	0,4	0,0431	95
10	0,3674	0,065	121
15	0,3743	0,0631	122
20	0,3474	0,0766	128
25	0,3356	0,0898	142
30	0,3376	0,0916	146
35	0,3473	0,0906	152
40	0,3535	0,0897	155
45	0,3492	0,0927	157
50	0,3511	0,0935	160
55	0,3646	0,0877	161

4.3.6 Sieve analysis of glass beads proppants

The samples tested were labeled as following:

- Glassbeads 400-800 H 1550139 (20/40);
- MEGALUX 850-1180 µm untreated 1550248 (16/20).

The sieve analysis was performed according to API RP-19C standard [14]. Seven sieves were used for the test. 120 g of each sample was taken and placed and the mass was recorded. Each sample was poured onto the top sieve, the stack of sieves was placed in the testing sieve shaker and was agitated for 10 minutes at 278 oscillation per minute. Figure 27 represents the set up.

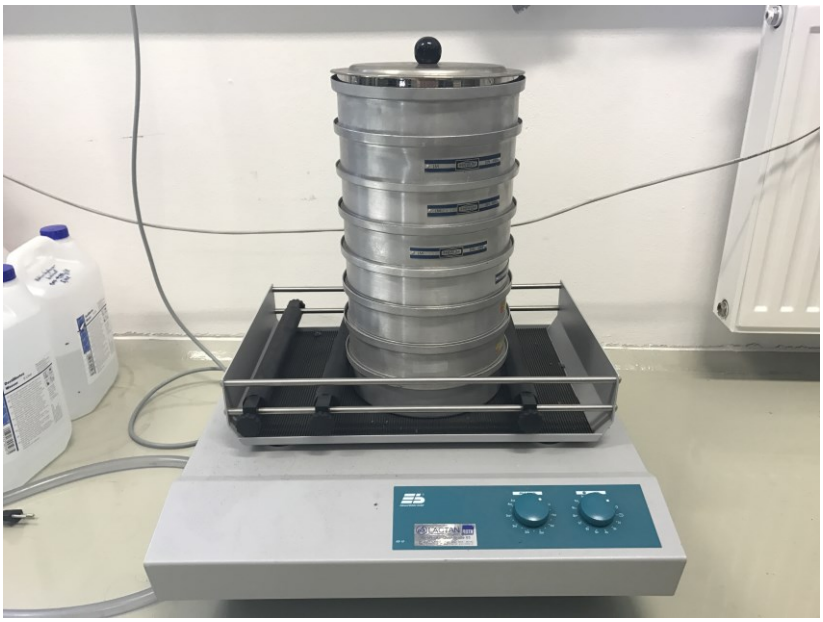

Figure 27: Sieve test set up

Upon 10 minutes, the sieve stack was removed from testing sieve shaker and the weight of the proppant left on each sieve and in the pan was measured and recorded. After that the cumulative mass was weighed and was confirmed to be within 0.5 % of the initial sample mass, as required per the standard.

The results of the sieve analysis in the form of grain size distribution is represented in Figure 28.

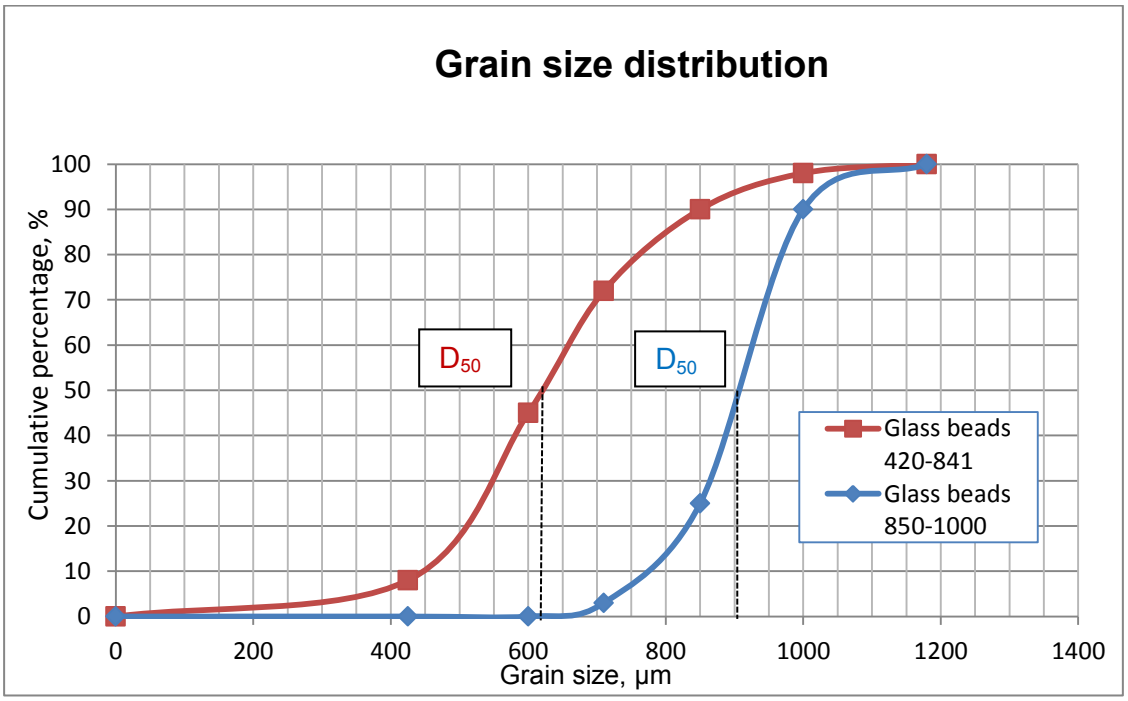

Figure 28: Grain size distribution for glass beads samples

In addition, the median diameter was obtained graphically. For glass 850-1000 μm glass beads d_{mean}=0.900 mm=0.0351 in; for glass 420-841 glass beads d_{mean}=0.610 mm=0.024 in.

4.3.7 Proppant pack conductivity test

The first accepted standard for measuring proppant pack conductivity is API RP61 “Recommended Practices for evaluating short-term conductivity of proppants”. However, the practice has shown that the short-term conductivities of a proppant pack are of a small value, due to the rapid conductivity decrease after a certain period of time. Therefore, API RP19 D “Recommended Practices for evaluating long-term conductivity of proppants” was developed and is now used in the industry.

The following parameters can be tested [15, pp.2-3]:

- Short-term conductivity according to API RP 61;
- Long-term conductivity between core plates;
- Turbulence factors of gas flow;
- Multi-phase flow parameters;
- Proppant flowback parameters.

A cell modeling a fracture is placed in a hydraulic press. The filtered 2% potassium chloride solution is preheated to reservoir temperature and pumped through the packed fracture face. This pressure is maintained on the fracture face, while the flow rate through the core is measured at different closure pressures in 1000 psi increments. At a fixed compression of the pack, the following parameters are measured: pressure difference, flow rate and fracture width. Conductivity of the pack is determined as the multiplication of the permeability to the fracture width, where permeability is calculated according to Darcy’s equation by **Eq.11**:

$$k = 16.67 * \frac{q*\mu*L}{\Delta P*A} \qquad (11)$$

k permeability [mD]

q flowrate [ft^3/s]

μ fluid viscosity [cP]

L length [ft]

ΔP pressure drop [psi]

A the cell cross section [ft^2]

The setup of the testing facility is represented in Figure 29 below.

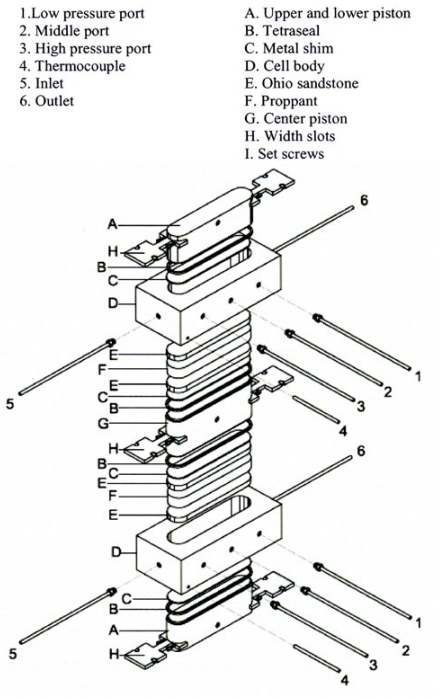

Figure 29: Prescribed test cell [15, p.3]

The apparatus includes the following elements:

- 10 inch. Square flow path;
- Filtered 2% KCl solution;
- Proppant loaded at volume equivalent to 0.25 in.width or 2 lb/ft^2;
- Proppant confined between sandstone cores (the standard Ohio sandstone core is used);
- In short- term conductivity testing the proppant is stressed for 15 minutes at each stress, in long-term conductivity testing the proppant is stressed for 50 hours;
- Stresses range from 1 to 14 KSI depending on the type of the proppant and its size;
- The test is conducted at temperature range of 150-250^{0}F.

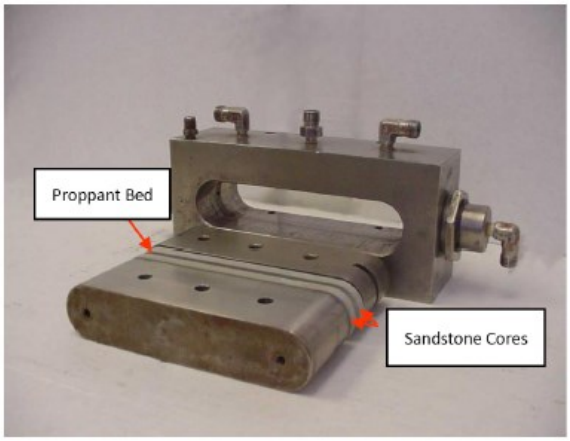

Figure 30: API conductivity test cell [15, p.5]

The conductivity test requires a special machinery that can withstand high pressures, it is expensive and it is normally performed by the special core laboratories, such as Stim-Lab, for instance. Due to these facts, it was not possible to perform this test in the university facilities on the Swarco glass beads. For the general estimation purposes, it was decided to use the corresponding data for the general glass beads, available in the published literature. The conductivity test data for glass beads of the mesh size 20/40 represented below has been taken from SPE-7573-MS.

Table 12: Glass beads (20/40) conductivity test data [16, pp.7-8]

Closure pressure (psi)	Conductivity (mD*ft)	Permeability (D)
2000	3123	150
4000	2603	125
6000	2082	100
8000	625	30
10000	250	12

4.3.8 Glass beads density tests

The density tests were performed by the third party company for the 400-800 μm glass beads with the Micrometrics 1340 Helium pycnometer and the following values were obtained. The test was performed on two samples of Swarco glass beads: untreated, hydrophobic.

Table 13: Glass beads density test [17, p.17]

Type	Density, g/cm^3
Glassbeads 400-800μm	2.4858
Glassbeads 400-800μm H	2.4851

5 Hydraulic fracturing treatment simulation

In order to evaluate the fluid and proppant efficiency, the hydraulic fracturing treatment was performed in GOHFER® software. The input data from the tutorial case for the vertical tight gas well was used.

5.1 Pretreatment data evaluation

The petrophysical data, the diagnostic fracture injection test (DFIT) results are evaluated in this chapter.

5.1.1 Well logging data evaluation

The well A was drilled down to 25000 ft MD (TVD) and was completed with 5.5 in. production casing. The well profile is vertical with zero horizontal offset. The wellbore inclination is 0^0, the wellbore azimuth is 360^0.

The potential hydrocarbon zone was confirmed with the logs. For this particular zone, the perforations were carried out in the interval of 11370 – 11411 ft. The total number of perforation shots are 20, the perforation diameter is 0.36 in.

The following logging services were run on Well A: gamma ray; resistivity; neutron porosity; density; ultrasonic caliper; sonic.

The data were imported to GOHFER® and processed. Poisson's ratio, permeability as well as volumes of sand, anhydrite, shale, limestone, dolomite and coal were obtained. The final processed logs for Well A are depicted on Figure 31, 32, 33.

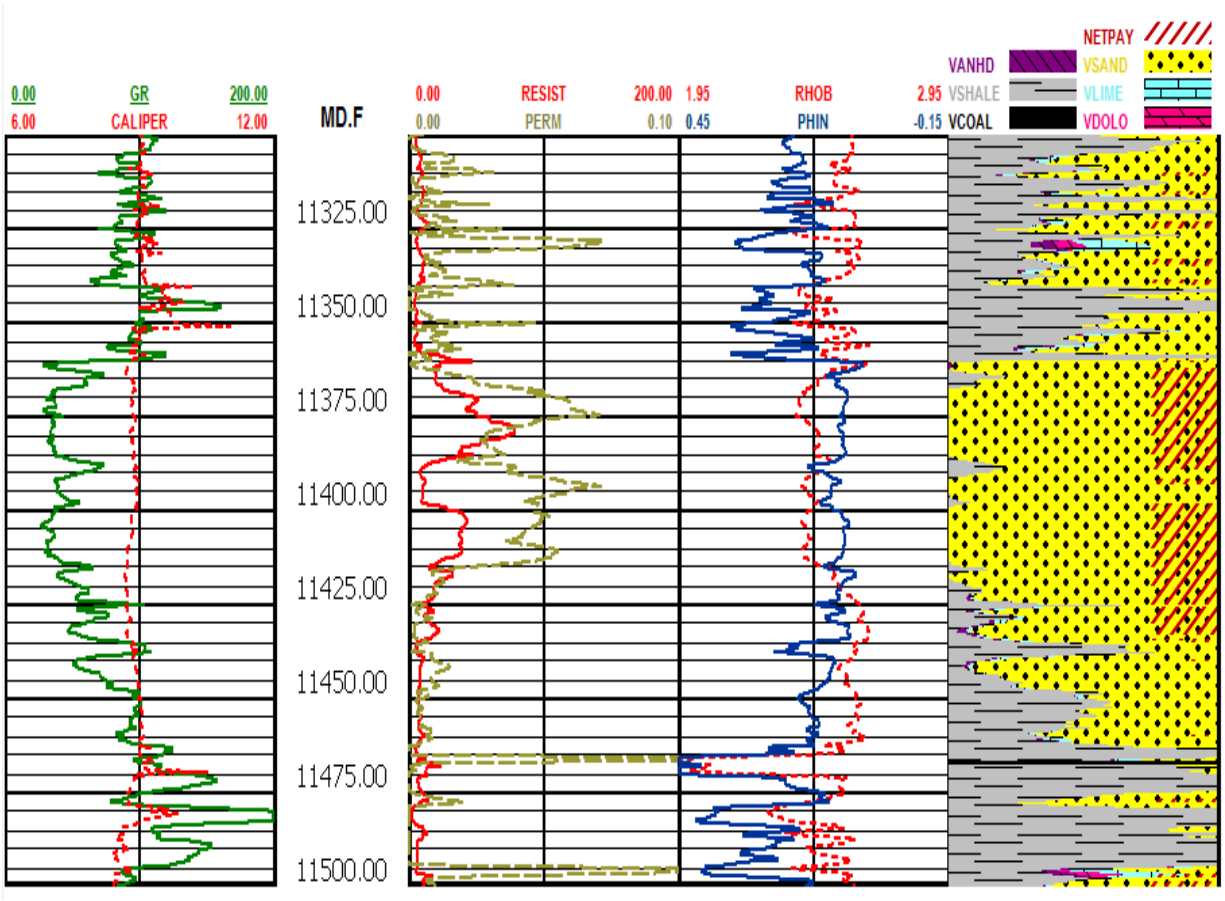

Figure 31: Formation evaluation data

The log has been cut down to the treatment interval depths for better visualization purposes. As it can clearly be seen from the log, the GR decreases, whereas Resistivity starts to increase at 11360 ft MD (TVD) depth. This behavior may be observed until the depth of 11475 ft MD (TVD) depth. This is a clear indication of the hydrocarbon-bearing formation. In order to identify, which type of fluid there is in the formation, the density (RHOB) and neutron porosity (PHIN) logs have to be analyzed. At the indicated interval, porosity starts to decrease significantly and density slightly decreases as well. These two curves cross over and this is recognized as a gas effect in petrophysics. As we can see from the lithology analysis, the zone of interest predominantly consists of sandstone.

In addition, in many gas plays , the synthetic and measured DTC curves may be used to help identify gas-bearing intervals. The synthetic DTC curves were derived from resistivity, neutron prosoity, average porosity and gammay ray data and are depicted in the log below. It is clearly seen, that the DTC curves start to separate in the considered area, indicating that the sandstone is gas-bearing.

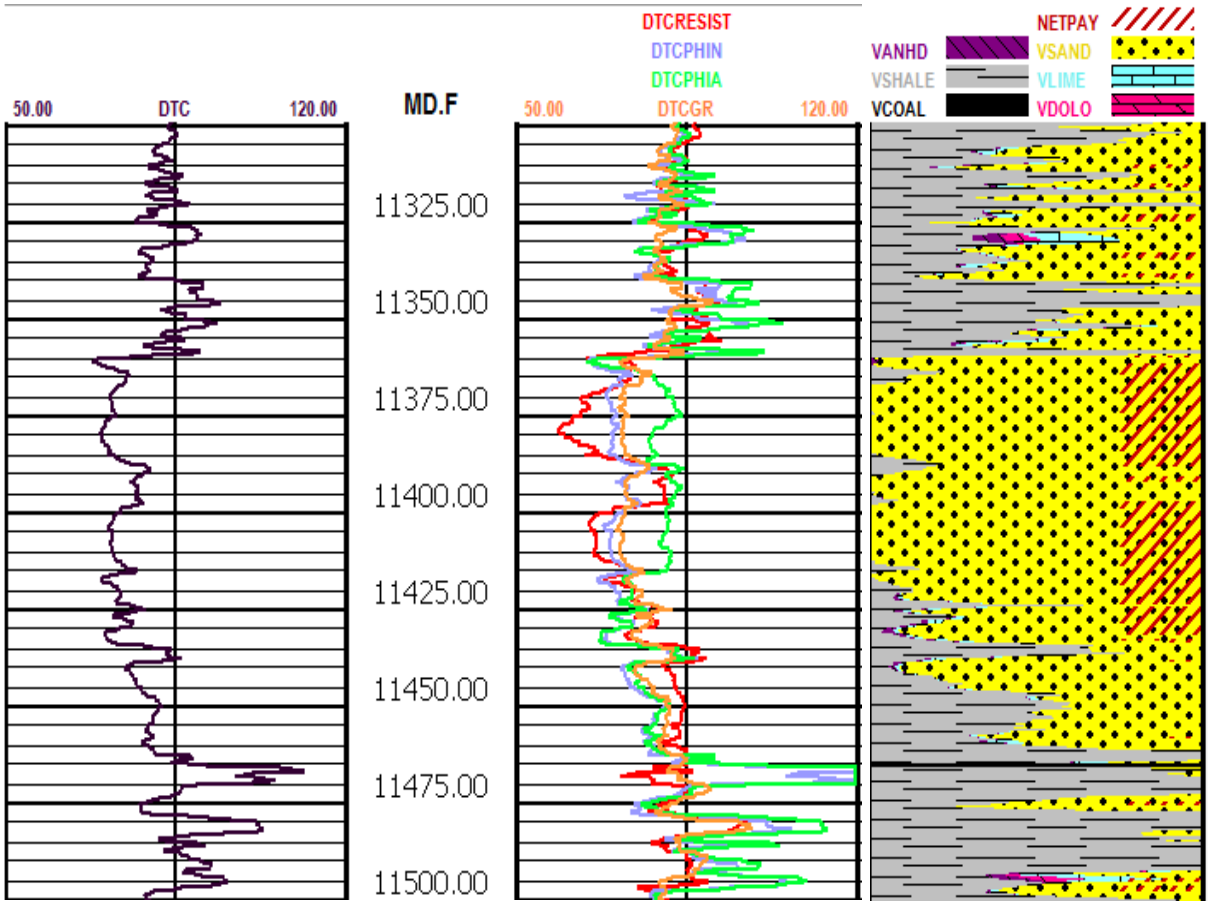

Figure 32: Sonic data analysis

Young's Modulus, Poisson's ratio, total stress and permeability data has been calculated from the petrophysics data and in represented in Figure 33.

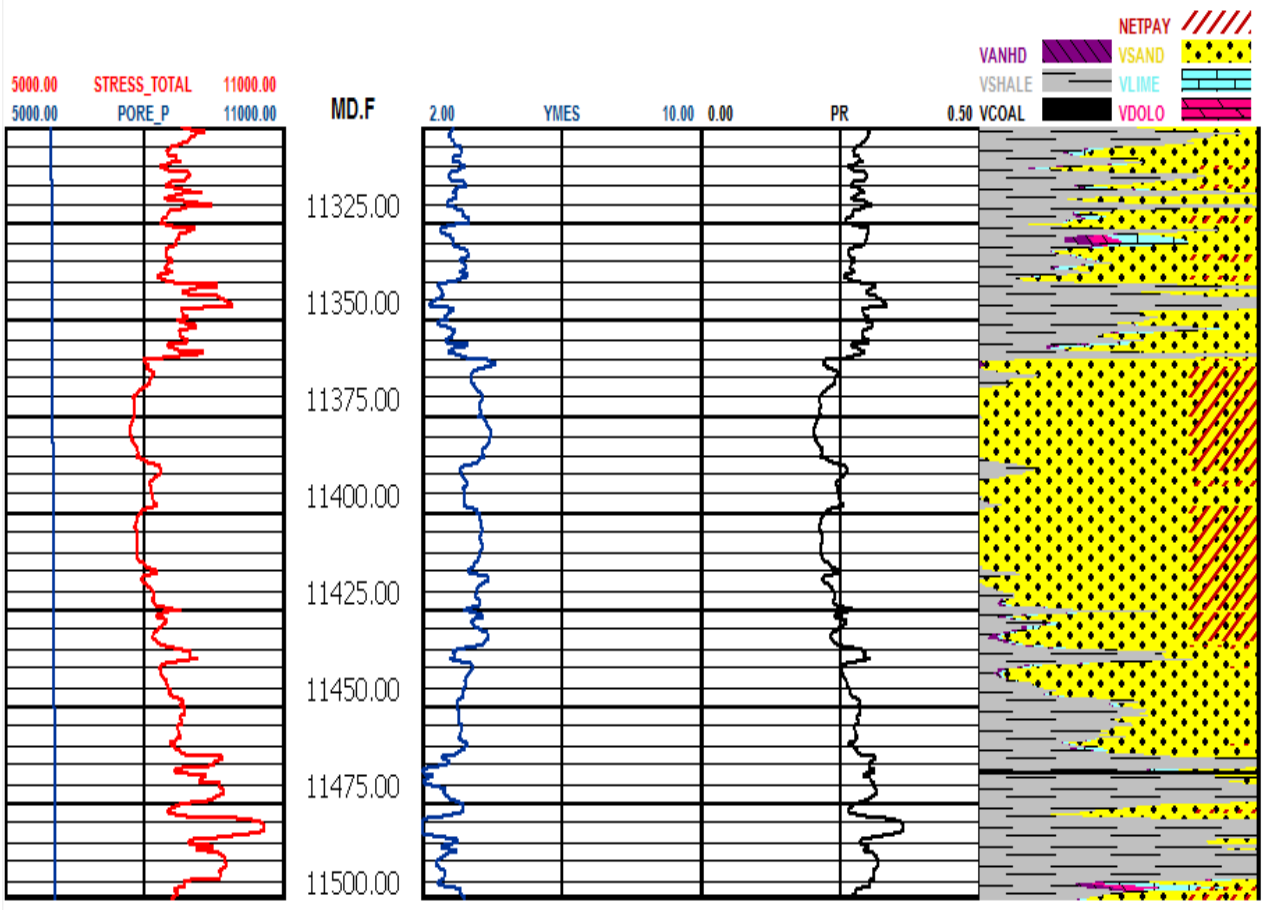

Figure 33: Derived geophysical properties

Permeability curve shows extremely low values with average 0.04 mD. Tight gas reservoirs are generally defined as the reservoirs with the matrix permeability less than 0.1 mD. Therefore, based on petrophysical data analysis, it is concluded that this is a tight gas sandstone reservoir.

Based on DTC input, the software evaluates the Young‘s modulus and Poisson‘s ratio values with the help of the synthetic correlations built in the program calculation algorithm. The total closure stress is calculated internally and is represented

5.1.2 Diagnostic fracture injection test (DFIT)

The diagnostic fracture injection test (DFIT) is normally performed prior to the main stimulation treatment. The intent is to break the formation to create the short fracture during the injection period, and then observe the closure of the fracture system during the falloff period. The purpose of diagnostic injection/falloff test or mini frac test is to provide the best possible information on the formation, in particular the identification of fracture closure pressure, fracture gradient, fluid leakoff coefficient, fluid efficiency, formation permeability and reservoir pressure. DFIT is performed only with the fluid, without proppants.

In low-permeability formations, the closure test is usually performed with a Newtonian, non-wall building fluid such as diesel or water containing 2% (weight to weight) of potassium chloride. In this case the DFIT was performed with KCL. The post-job diagnostics was performed in GOHFER®. The obtained data is represented on Figure 34.

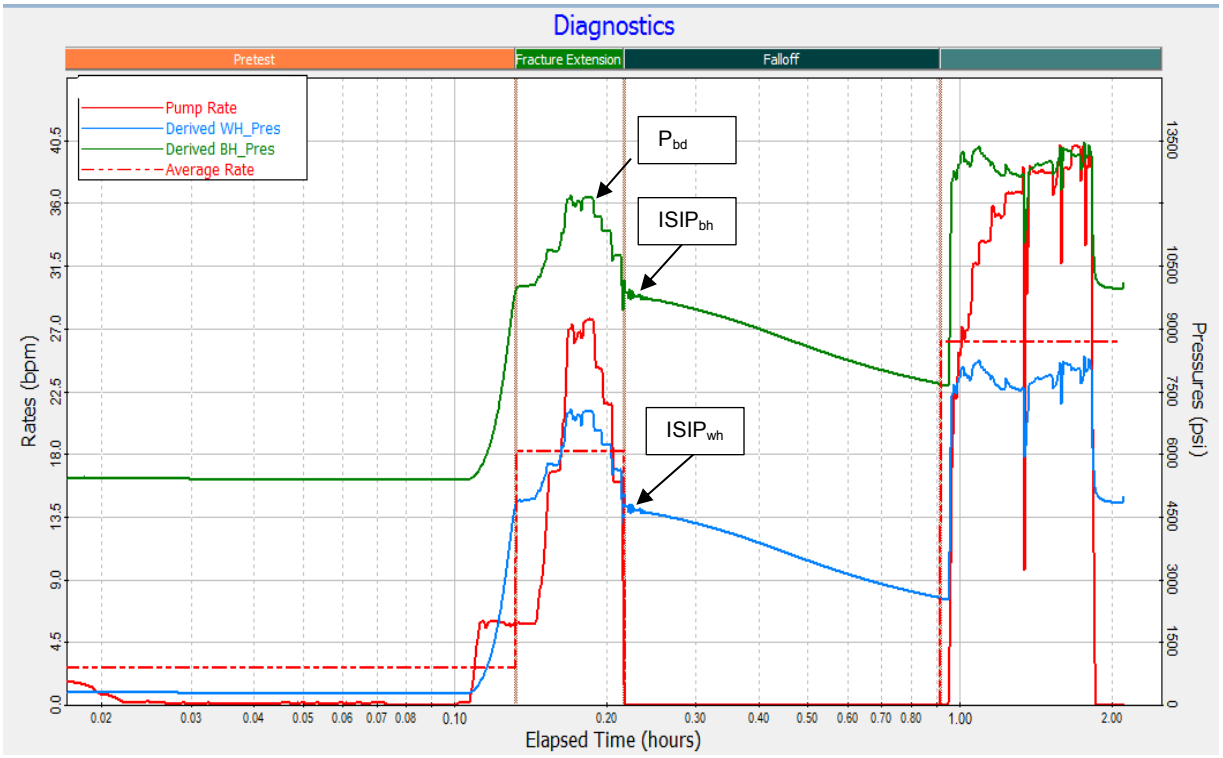

Figure 34: Minifrac post-job data

Three periods have been marked on the graph: pretest, fracture extension and falloff period. The initial pretest period duration was 6 minutes with the pumping rate equal to 3 bpm. After that, the pumping rate was increased to 18 bpm. During the fracture extension period the breakdown of the formation was reached. After 13 minutes of pumping, the well was shut-in and the pressure decline was observed for 47 minutes.

It may be concluded from the graph, that the bottomhole instantaneous shut in pressure (ISIP) is equal to 9844.36 psi, ISIP at surface is equal to 4729.23 psi. Based on this data, we can obtain the hydrostatic pressure of the fluid in the well and the friction pressures by **Eq.12**:

$$P_{hydr=} ISIP_{dh} - ISIP_{wh.} \qquad (12)$$

P_{hydr} hydrostatic pressure of the fluid [psi]

$ISIP_{dh}$ bottomhole instantaneous shut in pressure [psi]

$ISIP_{wh.}$ instantaneous shut in pressure at surface [psi]

$$P_{hydr}= 9844.36-4729.23=5115.13 \text{ psi.}$$

The sum of the surface friction pressure and friction pressure in pipes is equal to the surface pressure at the wellhead before the pumps shut down minus the $ISIP_{wh}$ **:**

$$P_{f\,pipes} + P_{f\,bh} = 5622 - 4729.23 = 895.77 \text{ psi}$$

The bottomhole friction pressure is determined as the bottomhole pressure before the pumps are shut down minus $ISIP_{bh}$:

$$P_{f\,bh} = 10730 - 9844.36 = 885.64 \text{ psi}$$

Therefore, the friction pressure in pipes is equal to:

$$P_{f\,pipes} = 895.77 - 885.64 = 10.13 \text{ psi}.$$

The breakdown pressure can be easily recognized by the change of the pressure slope at the constant rate. From the graph we may see that at the constant pumping rate of 18 bpm, the direction of the pressure slope changes, the point at which this process takes place denotes the breakdown. Therefore, the breakdown pressure at the bottomhole conditions is equal to 12000 psi.

Based on the calculated parameters, we can estimate the maximum treatment pressure at the moment when the breakdown occurs by Eq.5, mentioned in Chapter 2:

$$P_{si} = 12000 - 5115.13 + 10.13 = 6895 \text{ psi}.$$

In this particular case, the calibration injection test was performed directly before the fracture treatment, therefore, the data with the resembled pumping at the end of the falloff period corresponds to the beginning of the actual treatment.

From the graph, it may be seen that as soon as the pumps shut down, the pressure starts to decline. As soon as the fluid input into the fracture stops, the fracture will start to decrease in volume, as fluid is still leaking into the formation. As the fluid volume in the fracture (and hence the volume of the fracture itself) decreases, the fracture width also decreases until the fluid volume in the fracture is zero – the fracture has closed.

The time taken for the fracture to close defines the rate at which the leakoff is occurring, whilst the pressure at which the fracture closes (and the difference between the treating pressure and the closure pressure) tells us how hard it will be to produce the required fractures.

Pressure decline analysis after fracturing has traditionally been accomplished through some shut-in time-function. The G-function is a dimensionless time function relating shut-in time (t) to total pumping time (t_p) at an assumed constant rate. The concept behind this is that the pressure decline is the linear function of G. When represented on Cartesian plot, the decline pressure against G results is a straight line during the closure period with the slope equal to

the first pressure derivative (dp/dG) and y-intercept equal to theoretical pressure after shut-in. [18, pp.1-2]

The pressure decline behavior during closure in terms of the G-function and ISIP is represented in **Eq.13** [18, p.3]:

$$p(t) = ISIP - G(\propto_a, \propto_{c2}, \Delta t_D) * \frac{dP}{dG} \qquad (13)$$

Δt_D dimensionless time function

$\frac{dP}{dG}$ the first pressure derivative versus G

$\propto_a$ leakoff area parameter

$\propto_{c2}$ leakoff parameter during shut-in

Eq.14 [18, p.3]: describes the G-function in general form:

$$G(\Delta t_D) = \frac{4}{\pi} * (g(\Delta t_D) - g_0) \qquad (14)$$

g_0 computed value of G-function at shut-in

Dimensionless time function can be calculated by **Eq.15** [18, p.3]:

$$\Delta t_D = (t - t_p)/t_p \qquad (15)$$

t shut-in time [hrs]

t_p pumping time [hrs]

There are two limiting cases for the G-function. The first one is a low leakoff ($\propto_a$=1.0) or high efficiency where the fracture are open after shut-in varies approximately linearly with time. In this case the $g(\Delta t_D)$ is calculated by **Eq.16** [18, p.3]:

$$g(\Delta t_D) = \frac{4}{3} * \left(\left(1 + \Delta t_D\right)^{1.5} - \Delta t_D{}^{1.5}\right) \qquad (16)$$

The second case refers to the high leakoff ($\propto_a$=0.5) and low efficiency, in this case the fracture surface area varies with the square-root of time after shut-in and may be estimated by **Eq.17** [18, p.3]:

$$g(\Delta t_D) = (1 + \Delta t_D) * sin^{-1} * ((1 + \Delta t_D)^{-0.5} - \Delta t_D{}^{0.5}) \qquad (17)$$

The graphical representation of this technique is very fundamental and consists of simply plotting p (t) versus G. In case of ideal pressure decline behavior, G-function plot will result in the pressure decline data falling on a straight line during fracture closure pressure. When the decline pressure and G-function derivative G*dP/dG are plotted versus the G-function,

deviation of the derivative from the pressure decline data will help to identify the closure event.

Pre-closure analysis (PCA) was performed with the help of G-function analysis. The G-function is function designed to linearize the pressure behavior during normal fluid leakoff from a bi-wing fracture. A straight-line trend of the G-function derivative (G*dp/dG) is expected where the slope of the derivative is still increasing. In order to identify the closure pressure, the straight-line trend of G-function must be placed and the point where the G-Function derivative starts to deviate downward from the straight line is determined as the closure pressure.

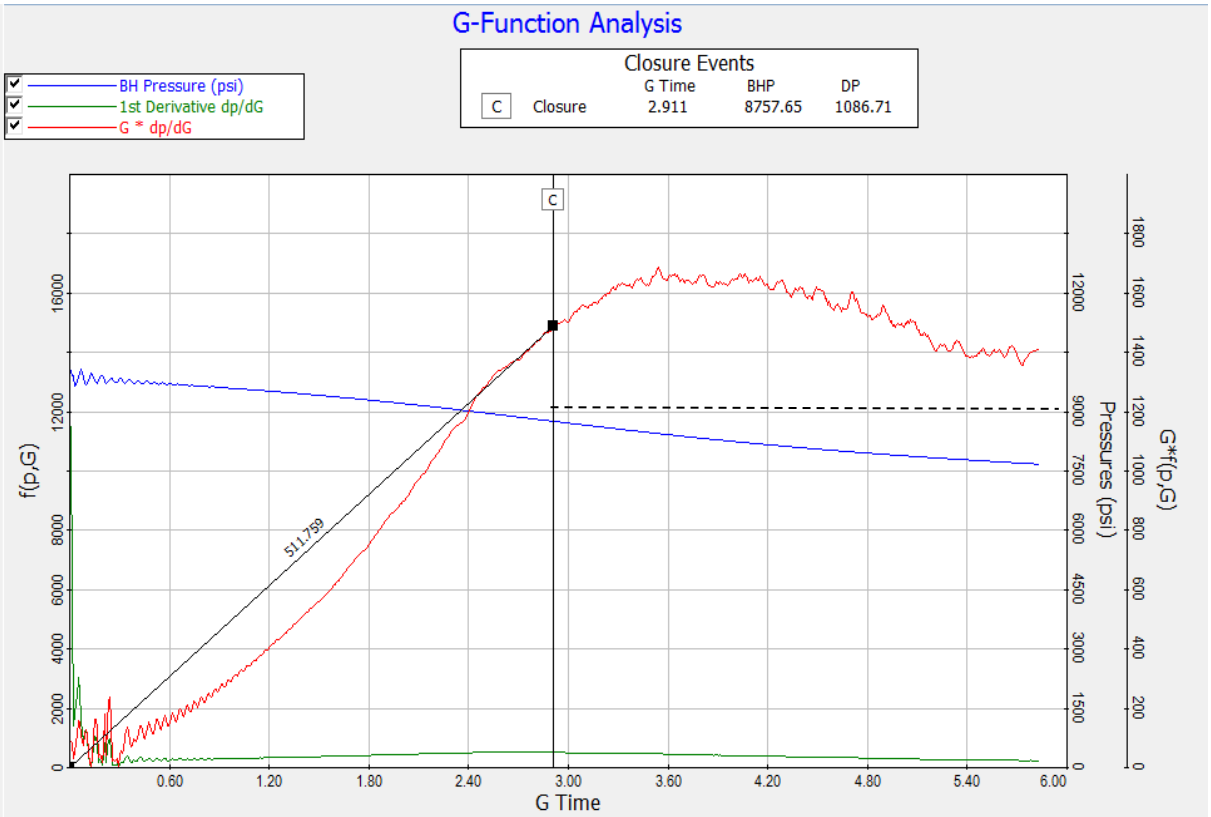

Figure 35: G-function analysis of pressure decline curve

Figure 35 displays the G function derivative (Gdp/dG) by red color, the first derivative of pressure dp/dG by green and the decline bottomhole pressure by blue. As it can be seen from this graph, the fracture closure occurs at G_c=2.911 and bottomhole closure pressure P_c is equal to 8757.65 psi, which corresponds to the blue line. Closure gradient of 0.7688 psi/ft is determined. The permeability at the treatment interval from G closure time is determined to be 0.046 mD. Net fracture pressure is determined as difference between ISIP and surface closure pressure and therefore is calculated by the following equation:

Net fracture pressure or process zone stress is calculated by **Eq.18** [19]:

$$\Delta p_{net} = ISIP_{bh} - P_c \qquad (18)$$

$$\Delta p_{net} = 9844.36 - 8757.65 = 1086.71\ psi$$

The obtained value corresponds to the DP value indicated in the top table on Figure 35.

Fracture gradient is calculated by **Eq.19** [19]:

$$\text{Fracture gradient} = ISIP_{dh}/\text{Formation depth} \quad (19)$$

$$\text{Fracture gradient} = 9844.36/11390.5 = 0.864 \text{ psi/ft}$$

Analysis of the Gdp/dG trend indicates that the derivative falls down a straight line,that extrapolates through normal leak-off data, exhibiting a concave up trend. This is recognized as the fracture height recession leak-off mechanism. In this leak-off mechanism the leakoff rate is small compared to the volume of fluid stored in the fracture, so the pressure decline is slow. As the fracture closes the remaining storage volume decreases and the leakoff rate accelerates with respect to the remaining compliant fracture volume and the pressure decline rate increases. The process is driven by a large storage volume of fluid in a fracture with out-of-zone growth across impermeable layers, which is applicable to the analyzed reservoir, as it is a tight sandstone.

Estimated reservoir parameters used for the simulation are represented in the Table 14 below.

Table 14: Estimated reservoir parameters

Parameter	**Unit**	**Value**
Net pay thickness	ft	65
Porosity	frac	0.1
Permeability	mD	0.046
Skin	dimensionless	5
Fracture gradient	psi/ft	0.864
Closure gradient	psi/ft	0.7688
Reservoir temperature	^{0}F	158
Reservoir pore pressure	psi	6249
Maximum surface injection P	psi	6895
Water saturation	frac	0.35
Gas saturation	frac	0.65
Gas specific gravity	sg	0.63

5.2 Hydraulic fracturing treatment design

The single fracture must be modelled and placed between top (11340 ft) and bottom barriers (11500 ft). Estimated geophysical properties from derived from the log are represented in Table 15.

Table 15: Geophysical properties used for fracture design

Parameter	Unit	Value
Poisson' ratio	dimensionless	0.25
Young's modulus	psi	3 500 000

The treatment string is placed in the wellbore. It has been assumed that there was a brine in the well prior to injection. The treatment string and fluid parameters are represented in Table 16.

Table 16: Wellbore treatment string and fluid

Measured	Treatment tubing	Effective treatment	Wellbore	Volume, gal
11480	11480	3.992	Brine	7464.18

The main peculiarity of the tight gas formations treatment is that the half-length of the fracture is a predominant parameter, that enhances the conductivity, and not the width, as it is in case of high permeability formation. Due to the low formation permeability in such formations, fluid leakoff also tends to be low. This has two consequences. First, pad volumes tend to be very low, relative to the rest of the job volumes. In some cases, a pad is hardly needed at all - the proppant-laden fluid can be used to create the fracture. The second consequence is that fracture closure time is long.

This means that the fracturing fluid has to suspend the proppant for a relatively long period of time at bottomhole temperature. Therefore, hydraulic fracture treatments in low permeability formations tend to have fairly large fluid and proppant volumes, although the overall proppant concentration in the fluid is relatively low. Fairly robust fracturing fluids, capable of maintaining viscosity for extended periods of time, must be used.

The goal of the hydraulic fracturing simulation is to achieve the following fracture parameters:

- Height – should be within barriers;
- Propped half length – preferably more than 250 ft (average statistical value for tight gas sandstone);
- Width – 4 to 8 diameters of the proppant grain;
- F_{CD} (dimensionless fracture conductivity) – from 1 to 10.

The main focus of this chapter was to develop the pumping schedule for the treatment, estimate the efficiency of the BEER® fracturing fluid and the glass beads proppants, based on the obtained fracture geometry parameters and the post-treatment production enhancement evaluation. In addition, the sensitivity analysis was performed in order to obtain the fracture geometry and production parameters for different proppants and make a comparison with the glass beads.

5.2.1 Fluid selection and BEER® fluid modeling in GOHFER®

Following the guidelines in subchapter 2.4, the hydraulic fracturing treatment design starts with the fluid selection. Based on Figure 36, the selection was performed.

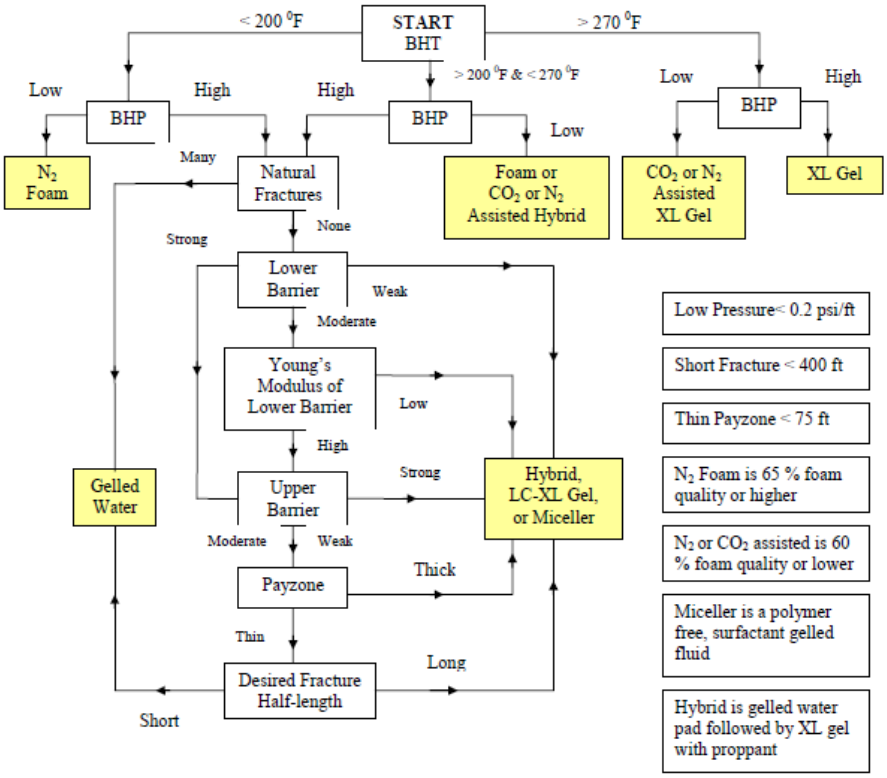

Figure 36: General guideline for fracturing fluid selection in tight gas wells [20, p. 110]

Figure 36 represents the flow chart for selection of the appropriate fracture fluid for the particular set of conditions. The following parameters influence the fluid selection: bottomhole temperature, bottomhole pressure, presence of natural fractures, type of lower and upper barrier, modulus of formation, height of the pay, desired fracture length.

For the field that is subjected to the analysis, the bottomhole temperature is less than 200^0F, the natural fracture could not be identified from the petrophysical data available, as wellbore images are necessary to identify those. Therefore, to simplify the case, it has been decided to assume that there are no natural fractures in the reservoir, the lower barrier is moderate. From the Figure 33 it can be seen, that Young modulus of the lower barrier is high, the payzone is considered to be thin, as it is less than 75 ft.

For the short fracture creation (less than 400 ft), it is recommended to use the gelled water, for the long fracture creation (more than 400 ft), it is recommended to use the crosslinked fluid.

In order to be able to test the BEER® fluid in the simulation, the first thing to do was to model its rheology in GOHFER®. The BEER® fluid is a gelled type of the fluid, it is not crosslinked, as it does not contain any crosslinker in its composition.
For fluid modelling, the laboratory rheology results were inserted into the software. Due to the limited capacity of the equipment in the university lab facilities, some of the parameters had to be assumed and estimated from the Aqua Master fluid, which was considered the most identical in terms of rheology. The list of the parameters are represented in Table 17.

Table 17: Parameters of fracturing fluid

Laboratory derived parameters	**Estimated parameters**
Viscosity versus time	Fluid cleanup rate =1.0
Power law exponent versus time	Fluid efficiency =65 %
Fluid consistency index versus time	Retained permeability = 64
Fluid density = 1.45 kg/l =90.52 lb/ft^3	Leakoff properties:
Test temperature =70^{0}C=158^{0}F	- spurt volume @ 1 mD, 1000 psi =0.0029 gal/ft^2
	- spurt volume @ 1000 mD, 1000 psi=1.00(gal/ft^2)
	- wall-building coefficient C_w @ 1 mD, 1000 psi, 180^{0}F=0.004 ft/min^0.5
	- wall-building coefficient C_w @ 1000 mD, 1000 psi, 180^{0}F=0.10 ft/min^0.5
	- dynamic leakoff coefficient C_d @ 1000 mD, 1000 psi, 180^{0}F=1^10(-4) ft/min
	- filtercake compressibility=0.2

The time based data of viscosity, power law index and fluid consistency index are represented in Table 11 in Subchapter 4.3.5.
Leakoff properties are used in order to match actual leakoff data through cores sample. Due to the absence of the test data, it was decided to leave the default values, as suggested in the manual.

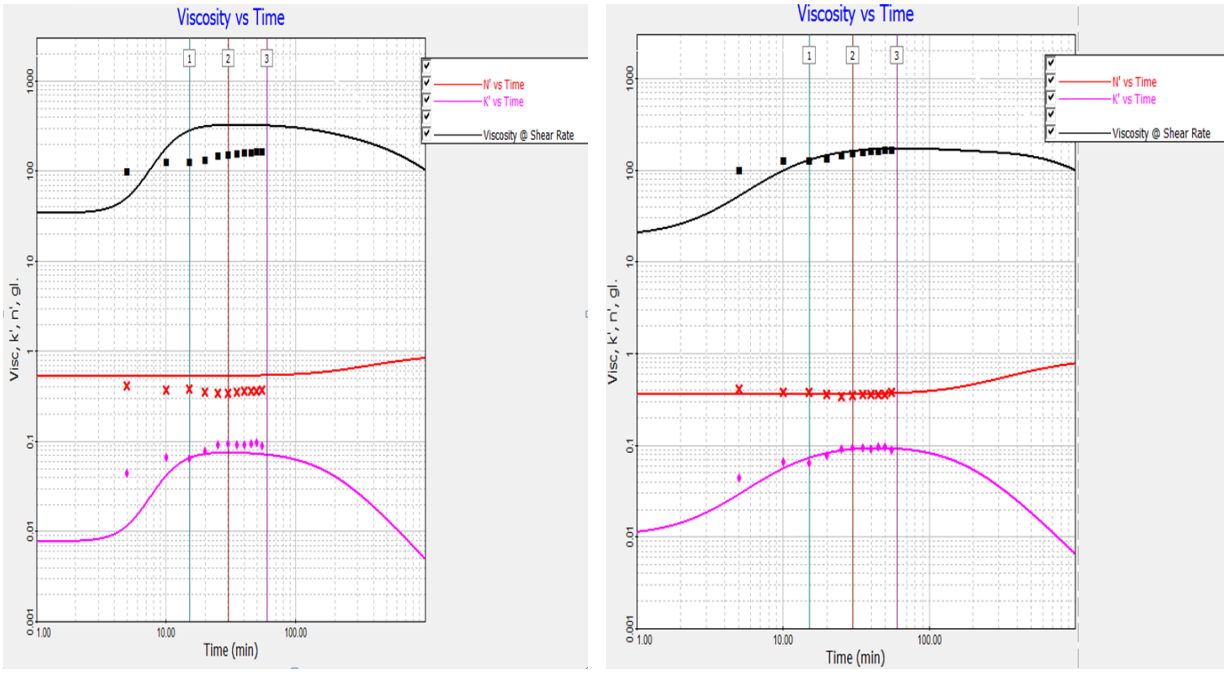

Figure 37: Imported data (one the left) and fitted rheology (on the right)

As it can be seen from the Figure 37, the color coded data (displayed as dots) are the imported data, whereas the solid lines represent the original data.
In order to accurately match the data, a series of curves fitting were performed:
-setting maximum K‘ and minimum n‘ values;
-fitting K‘;
-fitting n‘;
-fitting viscosity.

5.2.2 Proppant selection and modeling glass beads proppants in GOHFER®

Proppants are selected based on its permeability at the stress in the pay zone. Proppant permeability is also dependent on gel damage and non-Darcy effects.

The in-situ closure stress on proppant in the fracture is calculated by subtracting well flowing bottomhole pressure from the closure pressure by **Eq.20** [21,p.2]**:**

$$\sigma_{prop} = p_c - p_{wf} \qquad (20)$$

σ_{prop} closure pressure acting on proppants [psi]

p_c closure pressure [psi]

p_{wf} bottomhole well flowing pressure [psi]

Based on the production data available, the average bottomhole well flowing pressure is equal to 550 psi.

Therefore, $\sigma_{prop} = 8757.65 - 550 = 8257.65\ psi$

Taking into consideration the perforation diameter of 0.36 in and availability of glass beads size ranges, it was decided to analyze three types of proppant of 20/40 mesh size. Assuming a damage factor of 20%, taking into consideration the closure stress on proppant value and the perforation diameter, the following conventional proppants were considered and compared to each other:

- Jordan Unimin sand proppants 20/40;
- Low density ceramics Carbolite 20/40;
- Carboprop intermediate density ceramic proppant 20/40;
- Pre-cured atlas premium resin coated sand proppants 20/40.

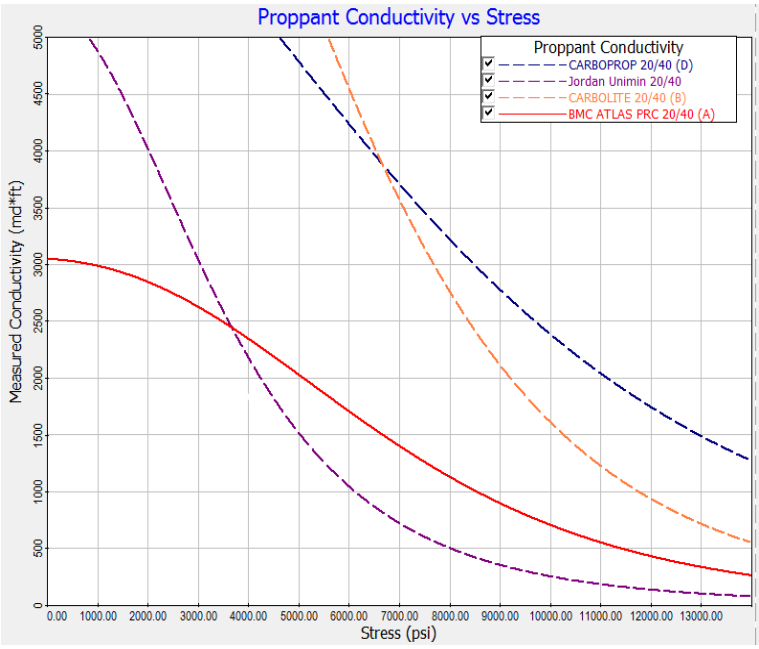

Figure 38: Conductivity data for different types of proppants

Figure 38 represents the conductivity of the different proppant types under various closure stresses, at the concentration of 2 lbm/ft^2. As it can be seen from the conductivity data analysis, at the estimated in-situ closure pressure on proppants equal to 8257.65 psi, the Carboprop intermediate density ceramic proppant shows the best conductivity values, slightly smaller conductivity under this stress is for Carbolite ceramics, pre-cured resin coated sand proppant shows the medium conductivity, whereas Jordan Unimin sand proppant shows the worst performance.

In order to estimate glass beads performance, the glass beads have been modeled in GOHFER® software. The software allows to generate the user-defined proppant when there is a limited conductivity data. It uses the generic correlations in order to compare the user defined proppant conductivity data with the expected performance of each generic type and size of the proppant.

The density, the mean diameter value and the conductivity data, described in details at Chapter 4, were imported to the software and based on this data the correlation was

performed. Based on the analysis of data, it has been concluded that the best correlation of the data is reached with the white sand. Figure 39 represents the results of the correlation for 20/40 glass beads.

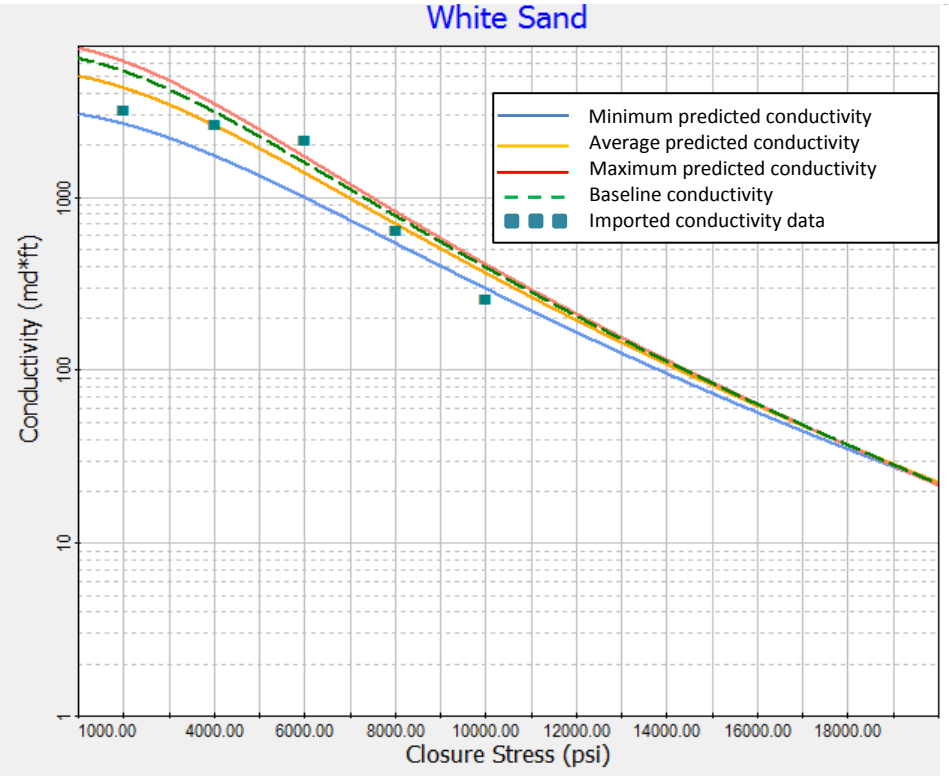

Figure 39: Glass beads conductivity data correlation

The correlation curves in the plot show the predicted conductivity for the minimum (blue), average (orange) and maximum (red) expected diameters. The baseline conductivity is depicted in green and the imported data is represented as green dots. It may be concluded from the graph that the data was entered correctly because it falls within the correlation curves.

As it can be predicted from the Figure 38 and Figure 39, at the expected in-situ closure pressure on proppant 8257.65 psi, the minimum estimated conductivity from the graph is equal approximately to 500 mD*ft. The selected proppants in this study are summarized in the Table 18.

Table 18: Selected proppants used in study

Proppant type	Proppant size	Proppant pack conductivity at 8257.65 psi, mD*ft
Jordan Unimin sand proppants	20/40	450
Carbolite	20/40	2250
Carboprop intermediate density ceramic proppant	20/40	2800
Pre-cured atlas premium resin coated sand proppants	20/40	1000
Glass beads	20/40	500

5.2.3 Treatment design

The next step in treatment design process is the treatment selection. It involves an examination of the sensitivity of the hydraulic fracture growth behavior, in order to identify the optimal pump rate and maximum treatment size.

Generally high injection rates should be considered because of the increased treatment efficiency resulting from decreased fluid-loss time and increased fracture width. In addition, the proppant carrying capacity is improved due to the increase of slurry velocity relative to proppant fall rates and a reduced pumping period, leading to less time for proppant fall and less viscosity degradation. The size of the treating tubulars and the corresponding friction pressure typically limit the injection rates as a result of tubing or wellhead pressure ratings. The increase in surface pressure increases the horsepower requirement and cost.

The sensitivity analysis was run in order to investigate the fracture geometry development for 10, 20, 30, 40 bbl/min with the use of BEER® fluid and glass beads.

Table 19: Sensitivity analysis of the fracture geometry parameters depending on different slurry rates

Slurry rate, bbl/min	Gross fracture length, ft	Proppant cutoff half length, ft	Width, in.	Height, ft	kfWf, mD*ft
10	2000	420	0.381	95	13
20	2000	420	0.432	110	13.37
30	1980	480	0.45	115	13.98
40	1960	460	0.46	115	13.93

It should be mentioned what is meant by gross fracture length and the propped fracture half-length in this case. Gross fracture length is the total hydraulically created fracture tip length. The proppant cutoff length represents the maximum length of the fracture available for the

flow. The proppant cutoff half-length is based on the fracture geometry and proppant distribution in the grid. These are inputs to the production model and not intended to represent the behavior of the fracture. [7, p. 690]

Therefore, we can see that the higher the slurry rate, the wider is the fracture and the height of the fracture is bigger. The fracture conductivity is also increasing with the slurry rate.

By analyzing the proppant concentration for different slurry rates, it may be concluded, that the proppant is not effectively displaced at 10 bbl/min, resulting in more uneven distribution and higher concentration of the proppant at the perforation area. The higher the pumping rate, the better the distribution of the proppants is.

As for the fracture geometry parameters, it can be concluded that there is not so much difference for the geometry parameters between the cases with 30 bbl/min and 40 bbl/min slurry rates. The effective infinite conductivity fracture length is even slightly higher at 30bbl/min.

In the provided dataset the wellhead pressure ratings data are absent, however, based on the example of the actual job design treatments, the designed flowrate was on average 30 bbl/min was used. Taking into consideration all these factors, it has been decided to use this flow rate for the treatment design schedule.

Selection of the optimal job size treatment is the next step in the design. For every fluid/ proppant system, there is an optimal hydraulic fracture length that gives the highest possible hydrocarbon recovery. The optimal fracture treatment is therefore calculated at this fracture length. The sensitivity analysis was run for different job treatment sizes on the basis of BEER® fluid and glass beads, as the primary goal of the study is to analyze their effectiveness. The results are represented in Figure 40.

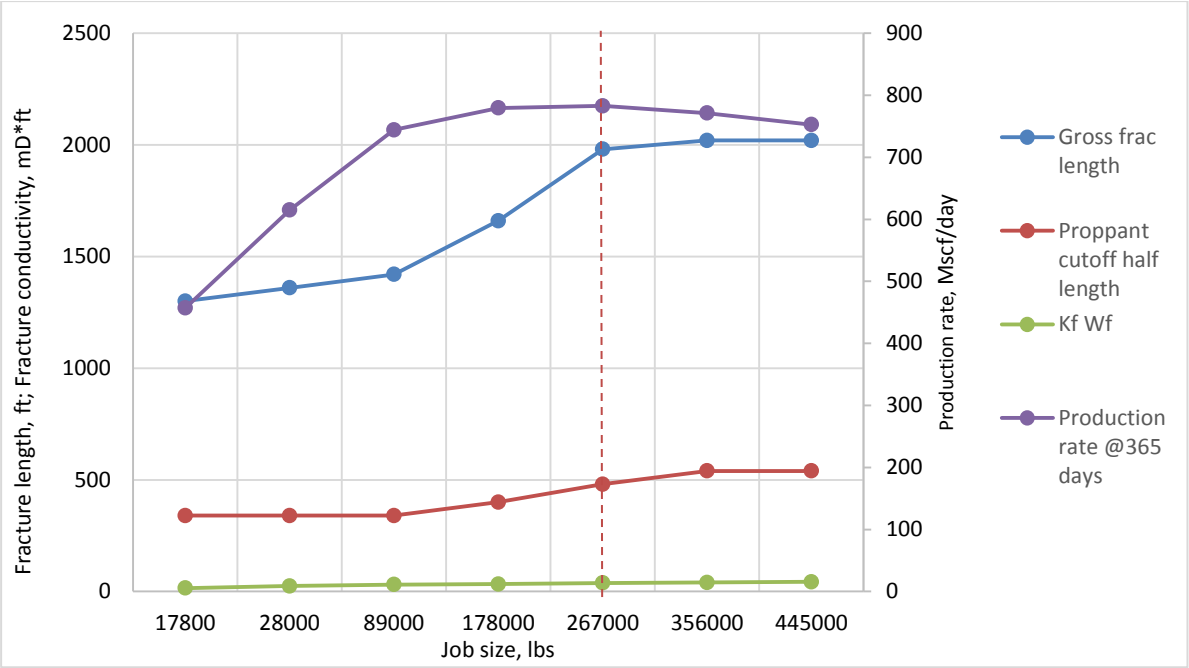

Figure 40: Sensitivity analysis of the fracture geometry properties and production rate based on job treatment sizes

As it can be seen from the graph, the job larger that 267000 lbs of proppants will not add significant gas production rates, on the contrary the production rate will be slighly lower. For the bigger job treatment sizes, the propped fracture length, the infinite effective fracture lenth and the fracture conductivity also stays almost the same. Therefore, it has been decided to subject 267000 lbs job treatment size for further analysis.

5.2.4 Treatment simulation in GOHFER®

The treatment pumping schedule is developed in order to provide a schedule for injecting the treating fluid and proppant. The schedule reflects the volume of fluid based on the desired penetration and viscosity profile and the mass and type of proppant based on the desired conductivity. Scheduling the proppant addition rate during the treatment is important. A major goal is to prevent such events, as undesired screenout, which might be caused by insufficient width, pad depletion, slurry dehydration near the wellbore resulting from a high proppant concentration. In practice, the proppant scheduling consists of the gradual incremental increases in proppant concentration during the course of the treatment.

The proppant concentration (pounds of proppant added to 1 gal of fluid, or ppg) in any segment of slurry increases because of fluid loss as the slurry moves down the fracture. The propped concentration in lb/ft^2 of fracture area depends on the rate of fluid loss from the slurry and the fracture width profile. The efficiency of the treatment determines the proppant addition schedule that will achieve a specific slurry concentration in the fracture at the end of pumping.

The pumping schedule with 7 stages was developed and represented in Table 20.

Table 20: Developed pumping schedule

Stage	Fluid type	Rate, bpm	Clean volume, gals	Proppant concentration, ppa
1 (Pad)	Slickwater	30	15000	0
2	Fracturing fluid	30	15000	0.8
3	Fracturing fluid	30	15000	1
4	Fracturing fluid	30	15000	2
5	Fracturing fluid	30	30000	3
6	Fracturing fluid	30	30000	4
7	Slickwater	30	8000	0

The slickwater was designed to be used in the pad and flush stages. At the stages 2-6 the crosslinked fluid is used.

Therefore, the total volumes of fluids and proppants are:

- Slickwater: 23000 gals total
- Fracturing fluid: 105000 gals total
- Proppant: 267000 lbs total

The designed pumping schedule is represented in Figure 41.

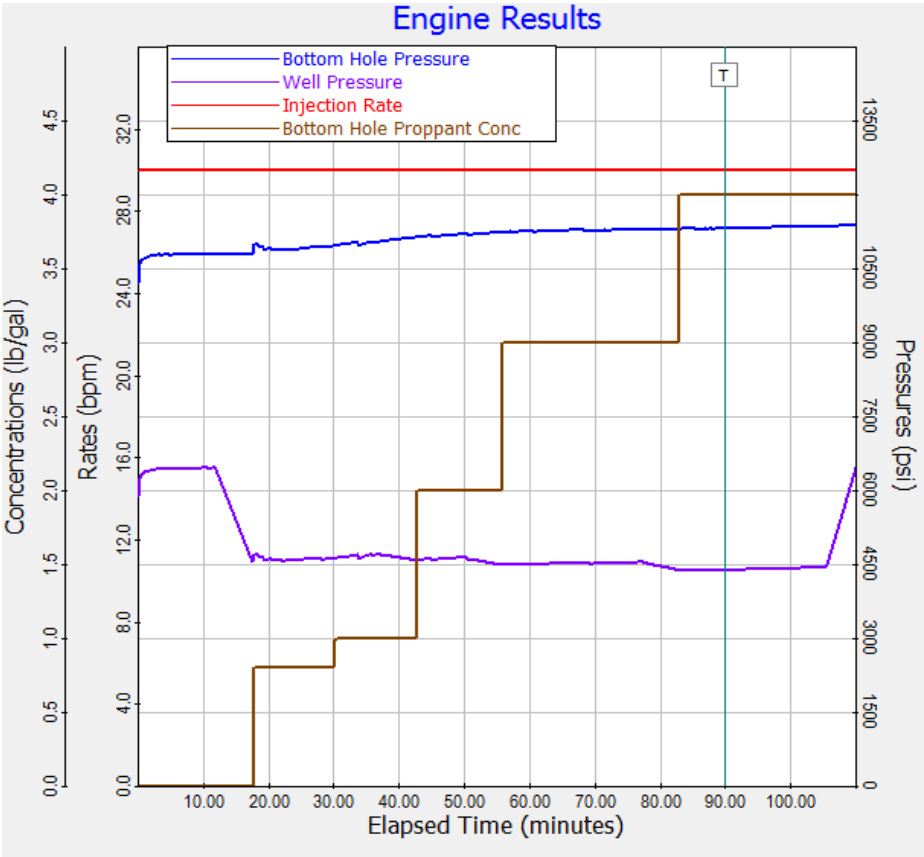

Figure 41: Designed treatment schedule

Based on the graph, it can be concluded that the maximum well pressure is 6500 psi, the maximum bottomhole pressure is 11500 psi.

The grid outputs below are the results of the simulation of the BEER® fluid and glass beads.

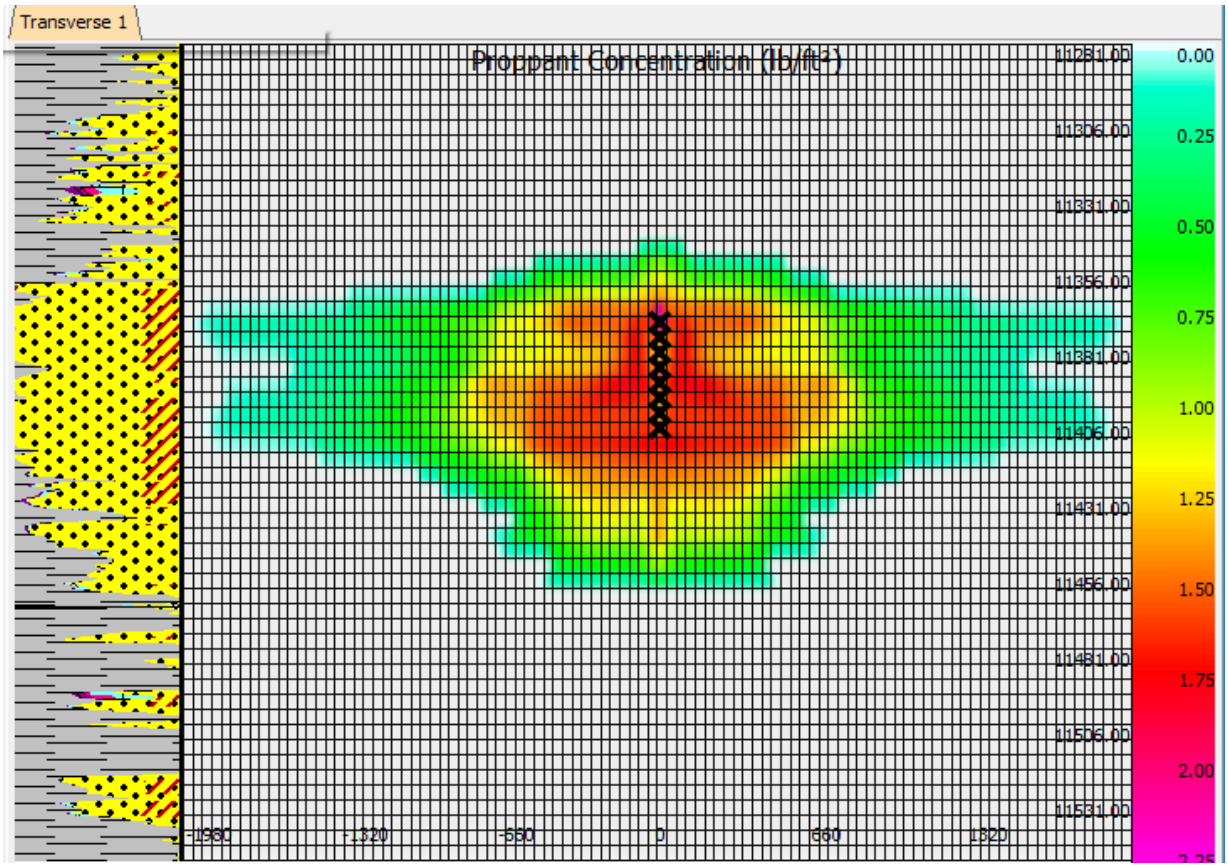

Figure 42: Proppant concentration distribution (Q= 30 bbl/min)

The average glass beads concentration based on the simulation results is 1.2 lb/ft^2. The perforations are represented on Figure 42 as the black crosses. From the graph we can see that the gross length is 1980 ft, the propant cutoff fracture half lentgth is 480 ft. The proppants are displaced quite evenly. The created fracture covers the whole net pay thickness.

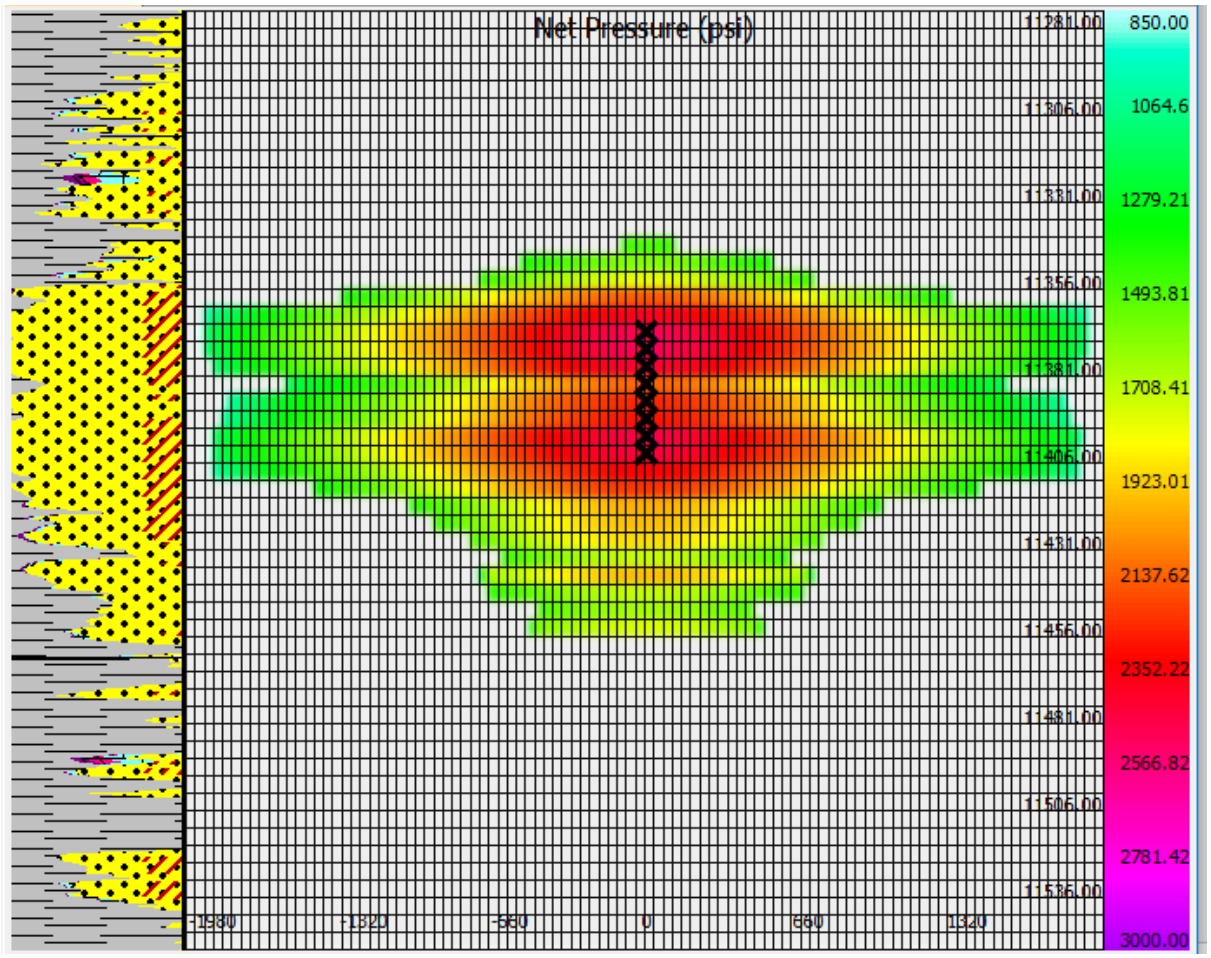

Figure 43: Net pressure distribution in the fracture (Q= 30 bbl/min)

Figure 43 indicates net pressure (pressure over closure pressure) at each node. A negative value indicates the pressure in the node is below closure stress. In our case the minimum value was calculated to be 62.04 psi and maximum value is 2464 psi. It has been mentioned earlier, that above the closure pressure the fracture will remain open, and below this pressure the fracture is closed. Therefore, it can be concluded that based on the obtained simulations, the fracture will remain open.

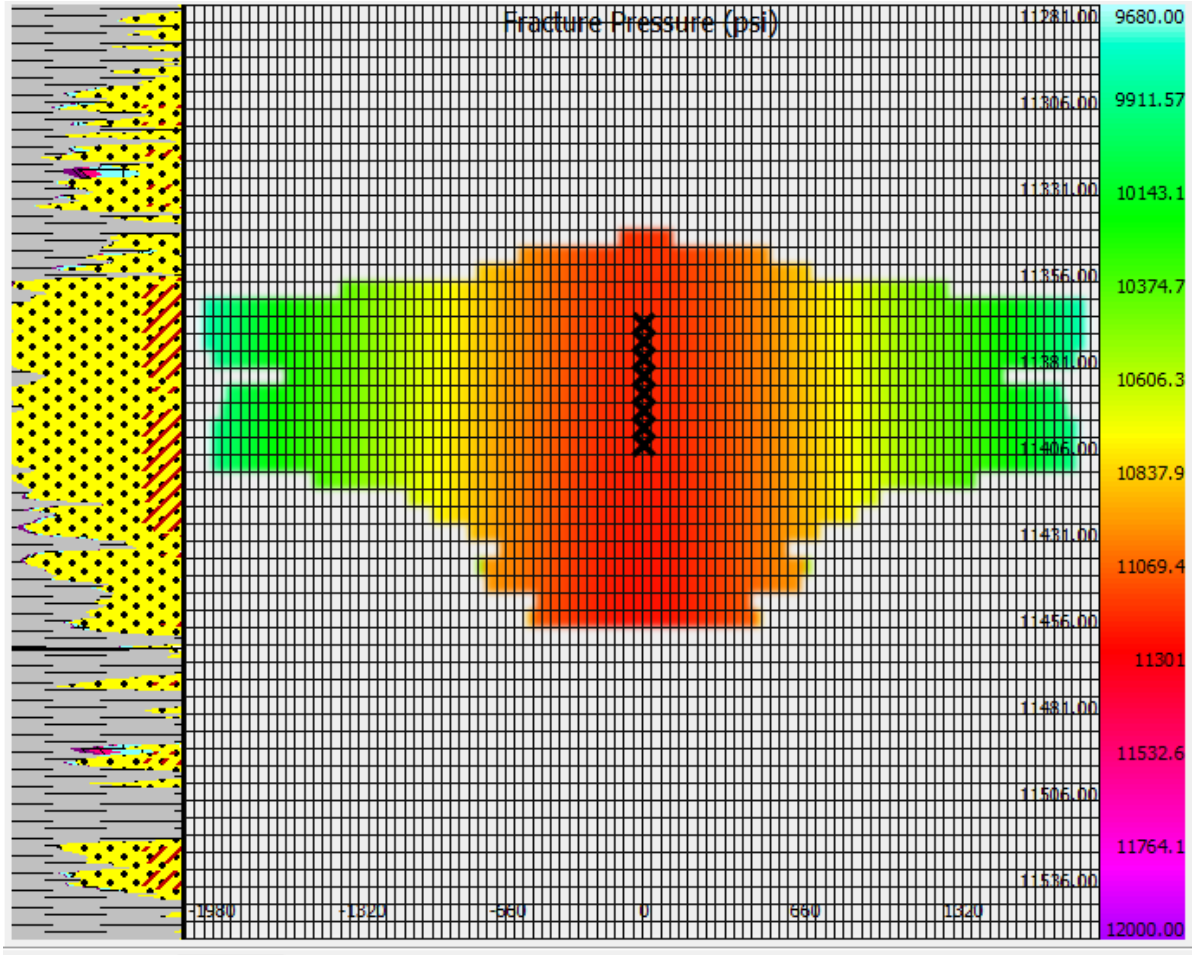

Figure 44: Fracture pressure distribution (Q= 30 bbl/min)

Figure 44 represents total fracture pressure at each node. As it can be seen from the figure, the maximum fracture pressure is concentrated at the near wellbore zone, the further the fracture propagation is, the less pressure is in the fracture. The maximum calculated value of fracture pressure is 11212 psi, the minimum value is 8871 psi.

5.2.5 Production prediction

The production prediction module was run in order to see the effectiveness of the designed treatment. The GOHFER® production model is a single phase Agarwal-Gardner type curve model with multiphase non-Darcy flow in the fracture. The following input parameters were used for the production input.

Table 21: Input parameters for production module

Wellbore radius	ft	0.325
Pipe roughness	in	0.0018
Production tubing inner diameter	in	3.992
Initil skin for unfractured well	dimensionelss	5
Drainage area	acre	40
Aspect ratio	dimensionelss	4
Constant flowing surface pressure	psi	300
Time period	days	365

The production calculations use the average prop concentration over the net pay and the closure stress, pore pressure, and reservoir properties as inputs to the conductivity. It gets a baseline with corrections for stress, and all other damages and then goes straight to the dynamic and multiphase losses. Once it has an estimated conductivity and formation deliverability, it uses the transient production model to get flow rate at each time. The time-dependent flow rate and frac geometry is used to get the Reynolds number in the frac that is used to update the damage and cleanup estimates. The model iterates at each producing time to get a new conductivity in balance with the current reservoir and well flow rates. The flowing length is determined from the damaged dynamic conductivity and reservoir flow capacity.

The model accounts for production interference between the adjacent producing fractures. The result of this is that the internal transverse fracs interfere with each other at a time determined by spacing and reservoir permeability. The benefit of the internal transverse fracs is primarily felt at early time and diminishes after interference is established. At late time, the bulk of the production occurs from the drainage areas of the outer fracs. At very long time, the entire composite wellbore can be modeled as an infinite-conductivity horizontal well of length equal to the total distance between the outermost fractures. The overall stimulation benefit can be represented by an equivalent wellbore radius equal to half the infinite-conductivity effective frac length established by cleanup. With more competing fractures the velocity within each frac decreases, if the entire well is production limited or if bottomhole flowing pressure (BHFP) increases due to friction or loading. This may decrease the effective length of the fractures because the energy available for cleanup is reduced.

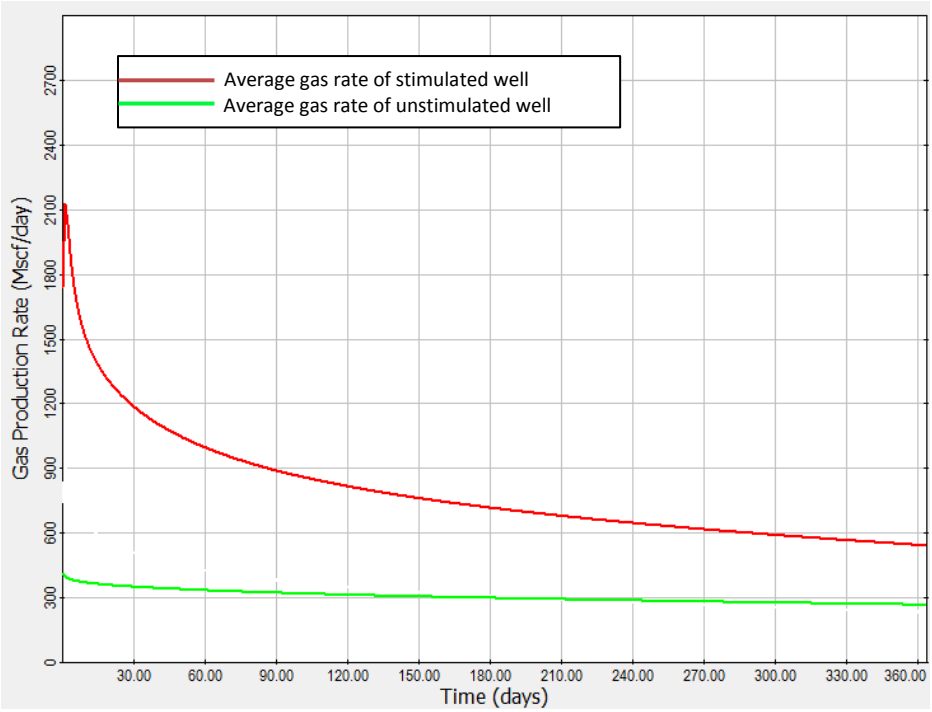

Figure 45: Average gas production rates of the stimulated and unstimulated wells (for 365 days)

As we can see from the obtained graph, average gas rate of unstimulated is depicted in red color. The post-treatment average gas production rate of the well is depicted in green color. We may see from the graph that for unstimulated well, the average gas rate is twice as low as for the stimulated well. The cumulative gas production is represented in Figure 46.

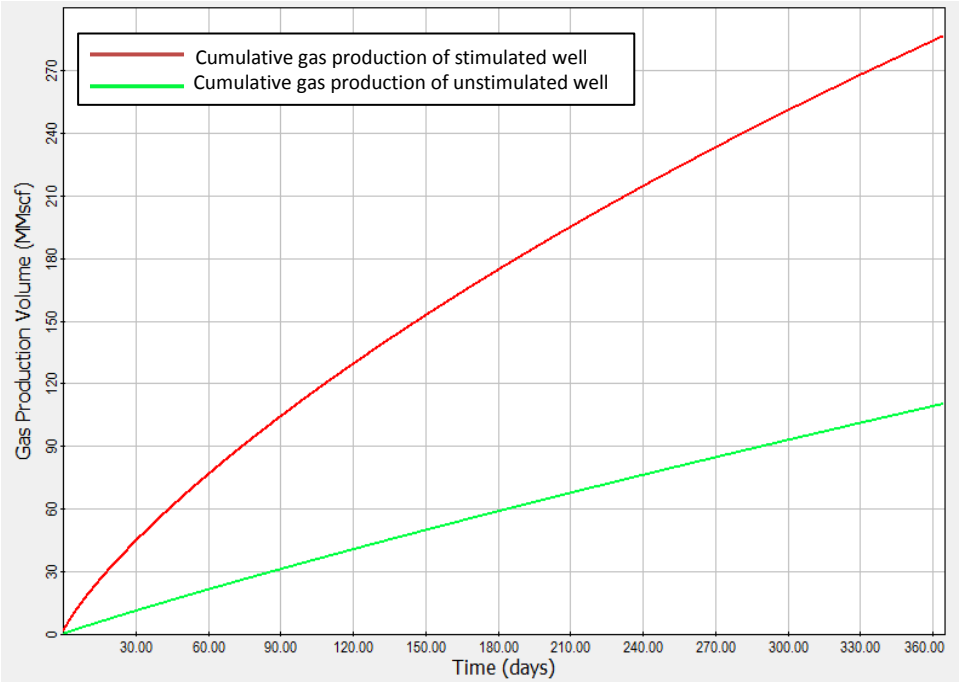

Figure 46: Cumulative production of the stimulated and unstimulated wells (for 365 days)

As it could be clearly seen from Figure 46, the cumulative production of the stimulated well is almost three times higher than the cumulative production of the unstimulated well.

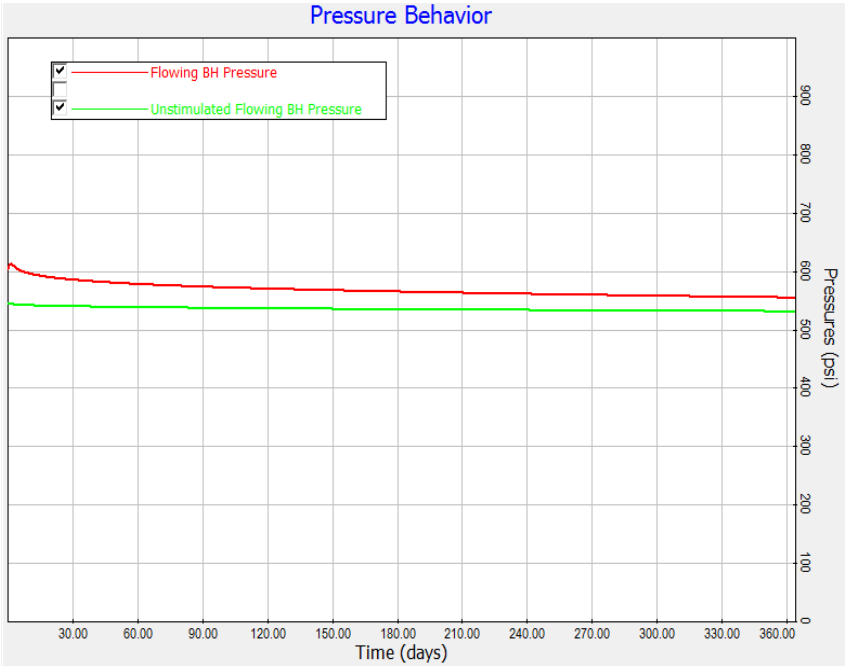

Figure 47: Flowing bottomhole pressure for the stimulated and unstimulated well

The flowing bottomhole pressure is approximately 550 psi for the treated well, for unstimulated it is equal to 525 psi.

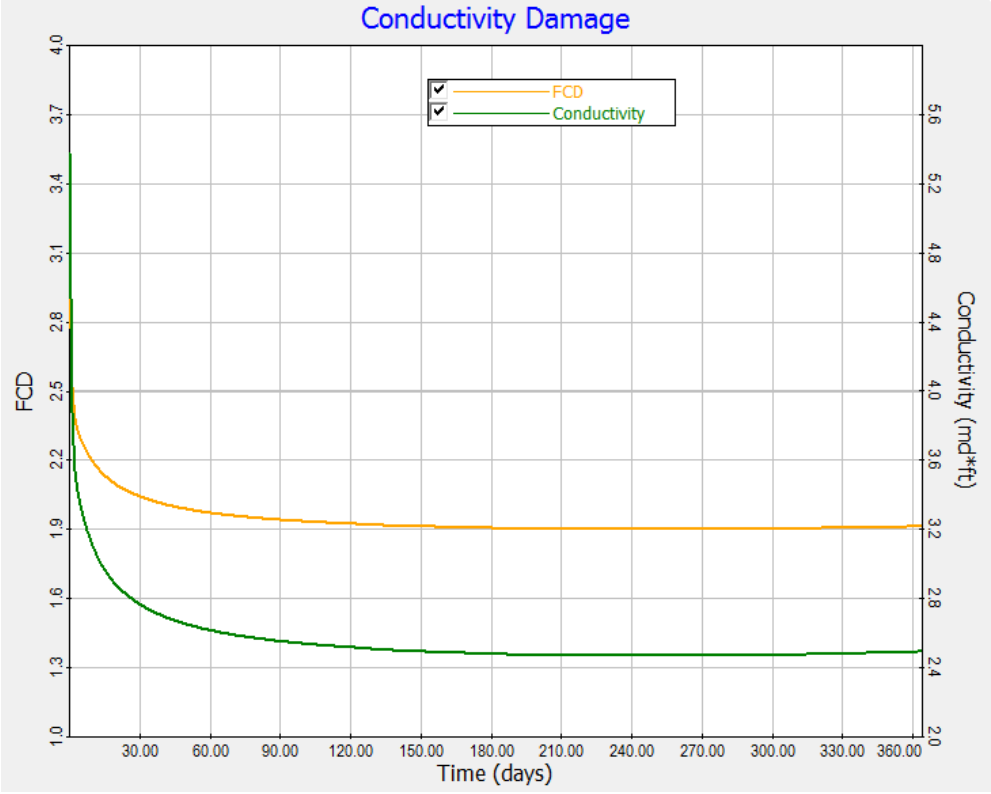

Figure 48: Conductivity damage results

On Figure 48, green refers to the fracture conductivity value k_fW_f, and orange to the dimensionless conductivity Fcd. Both values show the normal expected behavior and decrease with time.

The results of the production prediction are represented in Table 22 below.

Table 22: Production simulation results for one year period time

Parameter	Glass beads	RCP	Carboremamics	Carbolite	Jordan Unmim Sand
Peak rate, Mscf/day	2152.06	2149.67	2016.6	2177.19	1976.82
Final rate, Mscf/day	542.391	542.463	504.193	544.253	499.791
Final cumulative production, MMscf	287.672	287.671	268.102	289.339	264.898
Average Production rate, Mscf/day	788.143	788.14	734.526	792.71	725.749

5.2.6 Sensitivity analysis of the fracture and production model to different proppants

The rest of the proppants have been tested out and the obtained results were compared to the glass beads and are represented in the Table 23.

Table 23: Sensitivity Analysis of fracture properties for different types of proppants

Parameter	Glass beads	RCP	Carboremamics	Carbolite	Jordan Unmim Sand
Gross fracture length, ft	1980	1960	1980	1980	1980
Propped cutoff half-length, ft	480	460	480	480	460
Fracture conductivity, mD*ft	13.98	14.14	13.9	14.22	14.8

As it can be seen, the fracture model simulation gave almost the same results for all types of proppants, however, the proppant cutoff half-length for the resin coated proppant and for sand proppant is slightly less than for ceramics and glass beads. For the RCP and sand, this value equal to 460 ft, whereas for the glass beads and medium density ceramics, as well as carbolite it is equal to 480 ft.

As it can be seen, the fracture model simulation gave almost the same results for all types of proppants, however, the proppant cutoff half-length for the resin coated proppant and for sand proppant is slightly less than for ceramics and glass beads. For the RCP and sand, this value equal to 460 ft, whereas for the glass beads and medium density ceramics, as well as carbolite it is equal to 480 ft.

In addition, the production model was run and the average production rates and the cumulative production after 365 days upon treatment completion was compared and represented below.

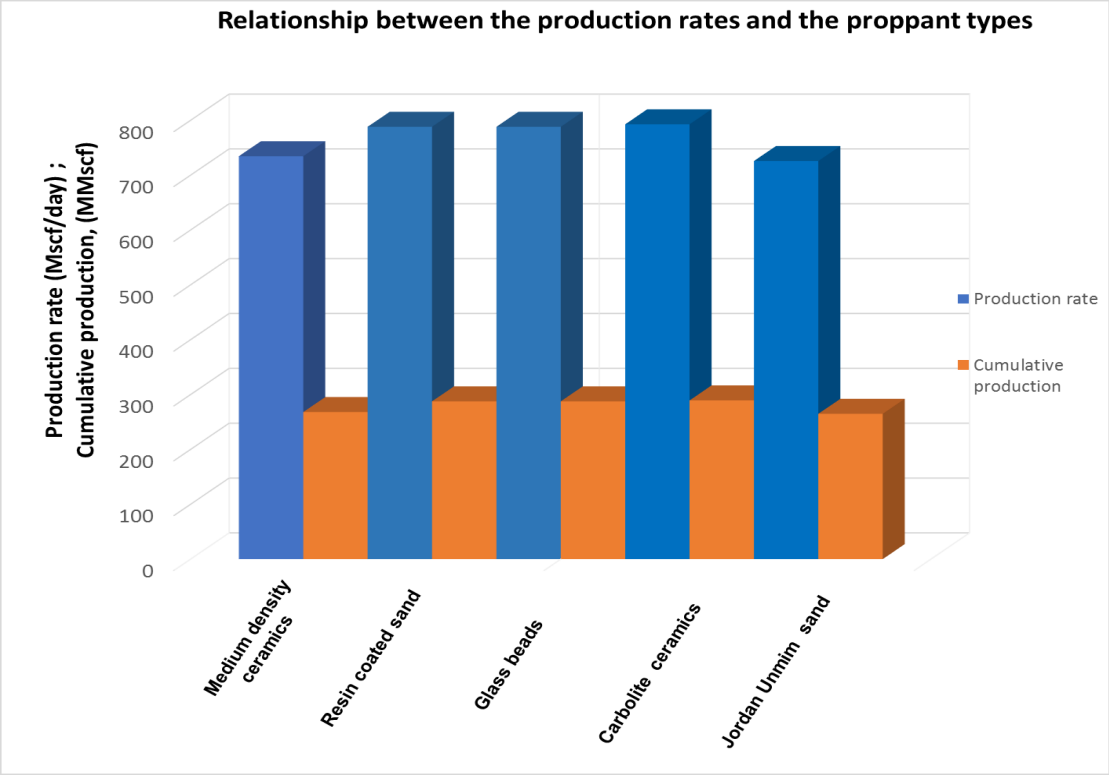

Figure 49: Production simulation results for different proppants (blue-cumulative production @365 days; orange- average production rate)

As it can be seen from Figure 49, in case if well is stimulated with medium density ceramics and Jordan Unmin sand , its average production rate and the cumulative production after 365 days are lower than for the cases, when RCP; glass beads and carbolite proppant are used This shows, that under these reservoir conditions, based on the used conductivity data and with all assumptions that were discussed previously, the glass beads show good results, comparable to carbolite and resin coated proppants.

All in all, the obtained results both for geometry properties and for the post-treatment production results are quite close and do not show a significant difference. Taking these into consideration, it may be concluded that the fracture model in the GOHFER® is more dependent on reservoir parameters and factors, such as Darcy effects, gel damage factors, wellbore cleanup rather than on only fluid rheology and the type of the proppant. This proves

that the software is based on the rigorous studies of the fracturing process and is really accurate.

5.2.7 Treatment simulation with the conventional fluid

In order to identify the effectiveness of the BEER® fluid application in such type of the reservoir, it has been decided to perform the same set of simulations for the conventional commercially available fluids with the glass beads being used as proppants. Two types of fluids have been selected for the comparison: Aqua Master and VISTAR fluid.

The same treatment schedule was run in the simulations, with the slickwater being used for the pad and overflash stages. The fracture geometry parameters, as well as the post-treatment production enhancement were investigated and compared.

Aqua Master is a gelled, non-crosslinked fluid. The basis of the gelled structure is guar. The rheology model of the selected fluid is represented in Figure 50.

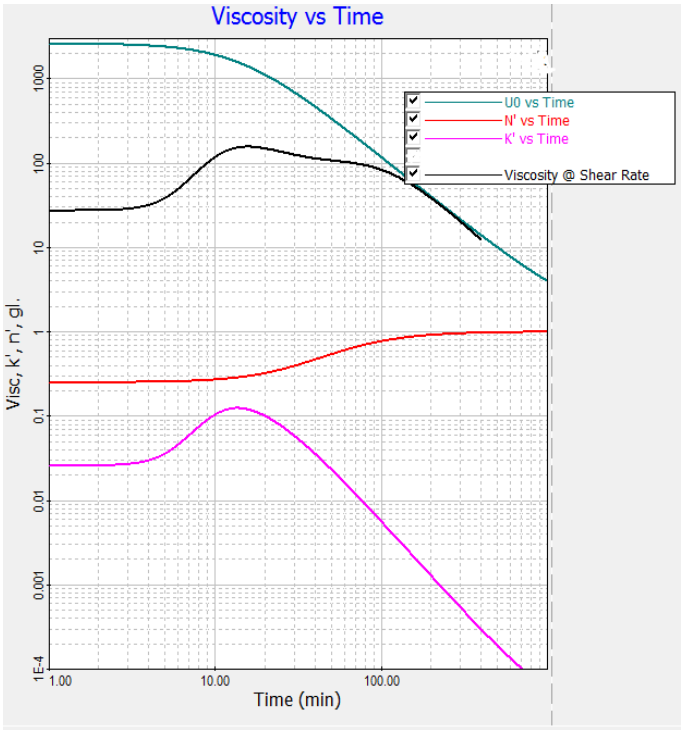

Figure 50: Aqua Master fluid rheology

The results of the simulations are summarized in the Table 24.

Table 24: Simulation results with Aqua Master fluid

Parameter	Glass beads	RCP	Carboremamics	Carbolite	Jordan Unmim Sand
Gross fracture length, ft	1980	2020	2020	2020	2020
Propped cutoff half-length, ft	460	460	460	460	460
Fracture conductivity, mD*ft	13.92	14.15	14.44	14.17	14
Average production rate, Mscf/day	786.103	790.99	795.96	793.79	789.88
Cumulative production @365 days, MMscf	286.928	288.71	290.53	289.73	288.31

As it can be seen from the simulation results, the proppant cutoff half-length is a little bit smaller in case when we select the Aqua Master fluid. In addition, the fracture will have the same geometry parameters, independent of the proppant type in this case. The production rates in this case will also be almost equal.

Baker Hughes Vistar fluid is a zirconate crosslinked system, designed so that only very low polymer loading is needed, as compared to other fluid systems. The base gel is a guarderivative (GW-45). The viscosity ranges of the selected fluid is considered to be similar to BEER® fluid and is represented in Figure 51.

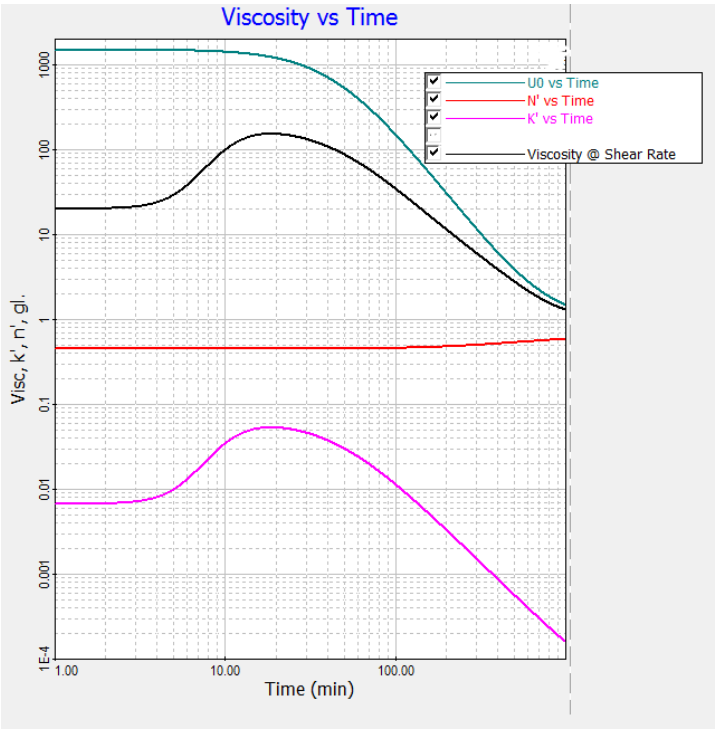

Figure 51: Vistar fluid rheology

The results of the simulations are summarized in the Table 25.

Table 25: Simulation results with Vistar fluid

Parameter	Glass beads	RCP	Carboremamics	Carbolite	Jordan Unmim Sand
Gross fracture length, ft	1900	1880	1880	1900	1880
Propped cutoff half-length, ft	520	500	520	500	500
Fracture conductivity, mD*ft	17.4	14.95	14.9	14.7	17.6
Average production rate, Mscf/day	797.84	797.5	797.52	798.83	797.194
Cumulative production @365 days, MMscf	291.21	291.1	291.10	291.57	290.98

As it can be seen from the simulation results, the propped cutoff half-length is higher in case when we use the crosslinked fluid, which corresponds to the expectations presented on Figure 36. An interesting observation is that in this case the propped half-length of the fracture with the use of the glass beads is equal to the case when carboceramics proppants are used. This could be due to the fact that they glass beads are better displaced with the crosslinked fluid.

Due to the bigger fracture length, the production rates that can be obtained after 365 days are slightly higher.

In order to compare the results, it has been decided to plot the propped half-length and fracture conductivity properties for all three designs with different fluid types with the glass beads being used as the proppant. The results are represented in Figure 52 and Figure 53 correspondingly.

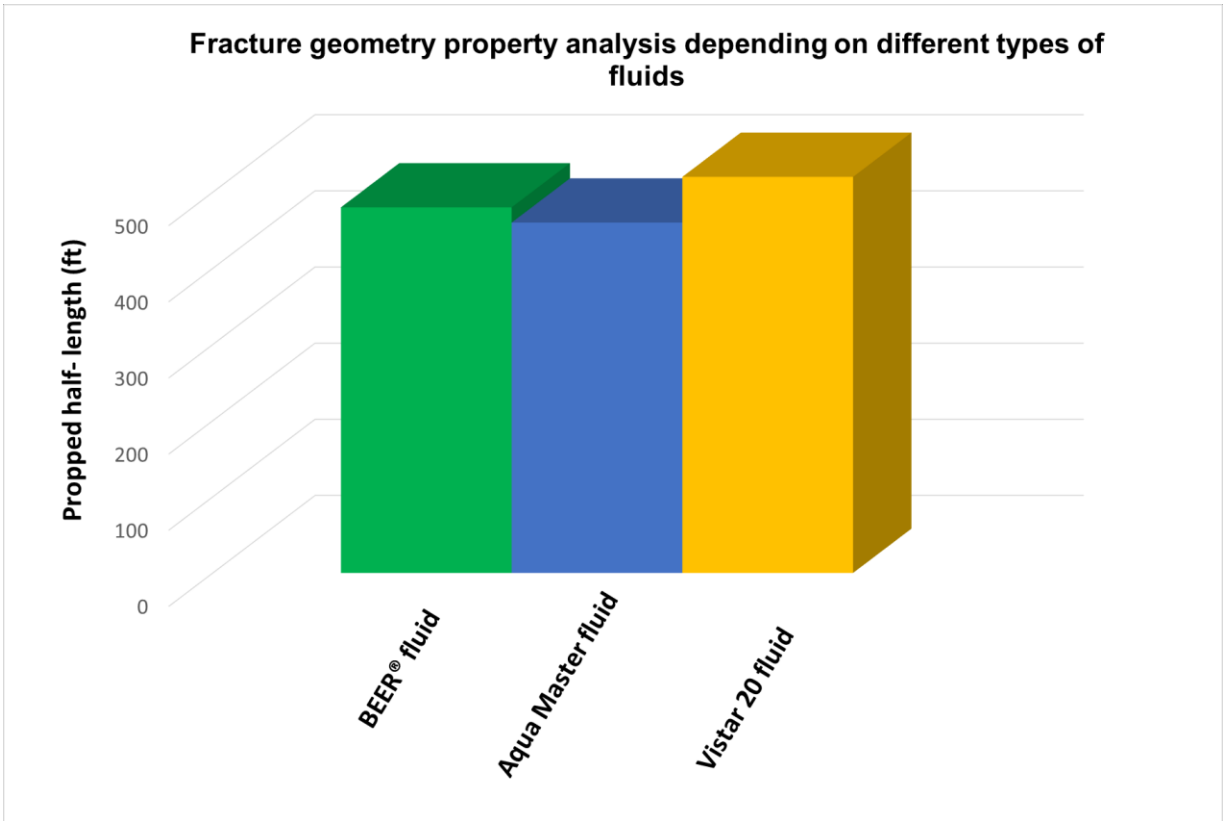

Figure 52: Propped fracture half-length of fracture for BEER®, Aqua Master and Vistar fluid Simulation

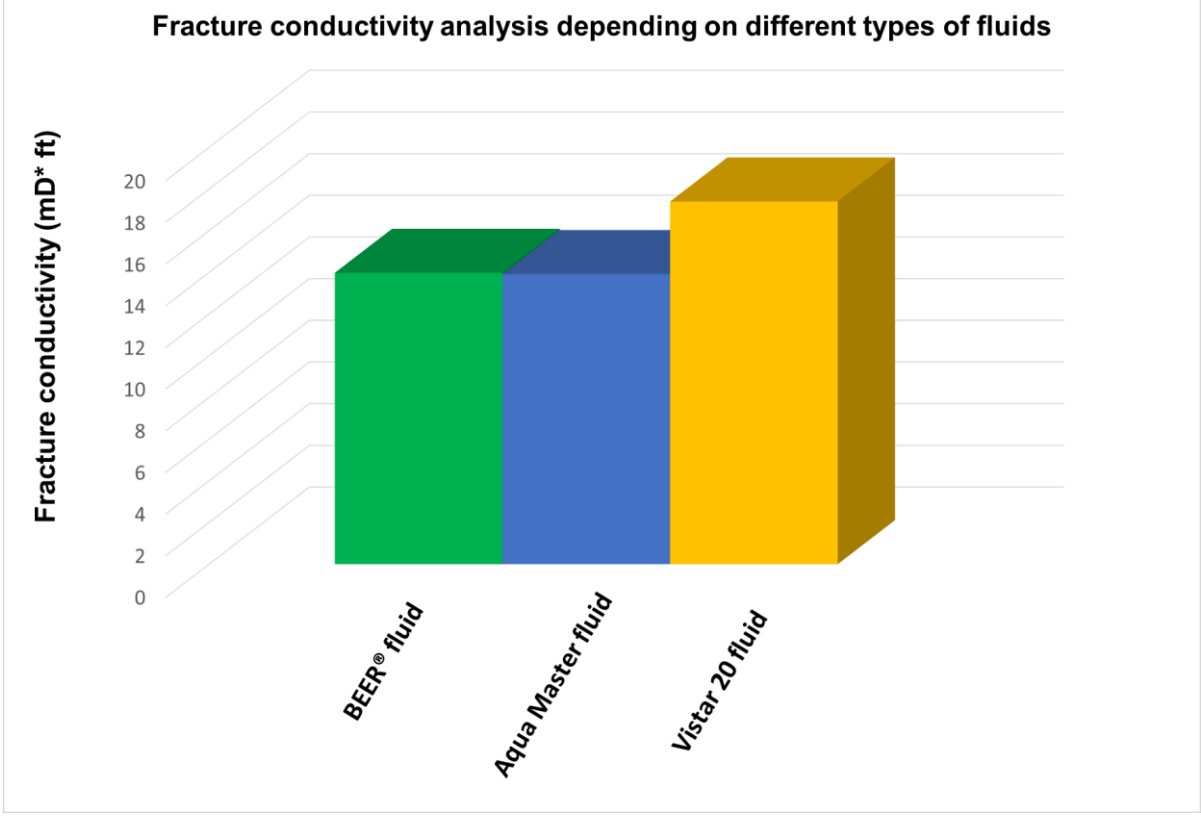

Figure 53: Fracture conductivity analysis for BEER®, Aqua Master and Vistar fluids

As it can be seen from the results, the BEER® fluid shows identical behavior to Aqua Master fluid. The obtained geometry parameters are within expected ranges for the linear gelled fluid structures. The crosslinked fluid shows a better behavior in terms of better proppant displacement and longer fracture half-length available for flow, as well as higher fracture conductivity, which is also confirmed by the literature review and is expected.

BEER® fluid performance has been cross checked with the performance of the commercially available fluid. The results are identical, hence, it proves the efficiency of the BEER® technology application for hydraulic fracturing stimulation in the considered reservoir under the analyzed conditions.

Conclusions and way forward

Based on the current work results, the following statements may be concluded:

1) Fracture width is directly proportional to volumetric injection rate. Increasing the injection rate serves to increase the net pressure, fracture volume and expands the fracture width.
2) Job size treatment and therefore, larger proppant volumes do not impact production such significantly due to the fact that there are other more important influencing factors that impact the ability of the formation to transit hydrocarbons through the fracture, such as reservoir pressure, gel damage, etc.
3) BEER® fluid technology is indeed suitable for hydraulic fracturing treatment of the analyzed reservoir, it provides good fracture geometry and also post-treatment production enhancement. Glass beads proppants performance was proved to be comparable to the resin-coated proppants and the light ceramics.
4) The simulation results of the treatment with BEER® fluid were compared to the conventional gelled fluid and were confirmed to be identical. This proves that the behavior of the proposed technology in such a complicated reservoir geology is within expectation. The results that were obtained for the simulation with the crosslinked fluid are better in terms of longer propped fracture half-length and higher fracture conductivity. Therefore, under these reservoir conditions crosslinked fluid might be the preferred option.
5) GOHFER® allows to model the user defined fracturing fluid and the proppant. Based on the generic correlation, modeled in the software, it can predict the proppant pack conductivity behavior even with the limited conductivity data.
6) GOHFER® is an integrated geomechanical fracture design tool, which means it uses a multi-disciplinary approach. It is capable to perform logs processing and pressure diagnostics, to model the treatment schedule and simulate the fracture geometry, to predict production behavior after the treatment performance. It also allows to perform an economic (NPV) analysis to compare different designs, however, this was out of scope of the current work.
7) GOHFER® has a user friendly interface and very good supporting documentation, such as manuals and presentations with the detailed explanation of the software features.

The way forward would be to perform the leakoff test on the BEER® fluid through the core sample and obtain more precise parameters for spurt volumes, retained permeability and the gel loading. In addition, it would be very beneficial to test out the glass beads proppant pack for the conductivity behavior. This would help to get more accurate results for the simulations.

Nomenclature

V_i volume of fluid leaked off into formation [ft^3]

C_{eff} fluid leak-off coefficient [$ft/min^{1/2}$]

A surface area of the fracture [ft^2]

t the time that the fracture was open [min]

E fluid efficiency [frac]

V_i volume of fluid leaked off into formation [ft^3]

V_t total volume of fluid pumped into formation [ft^3]

P_c closure pressure [psi]

v Poisson's ratio

α_v vertical Biot's poroelastic constant

α_h horizonal Biot's poroelastic constant

P_p pore pressure [psi]

ε_x regional horizontal strain, microstrains

E Young's Modulus [psi]

σ_t regional horizontal tectonic stress [psi]

P_{net} net pressure [psi]

P_{bht} bottomhole treating pressure [psi]

P_{nwb} near wellbore pressure [psi]

P_c closure pressure [psi]

P_{si} surface injection pressure [psi]

P_{bd} breakdown pressure [psi]

ΔP_h hydrostatic pressure drop [psi]

ΔP_f frictional pressure drop [psi]

F_{CD} dimensionless fracture conductivity

k_f fracture permeability [mD]

w fracture width [ft]

k formation permeability [mD]

x_f fracture half-length [ft]

$\Delta N_{p.n.}$ predicted annual incremental cumulative production for year n [ft^3]

$N_{p.n}^{f}$ forecasted annual incremental cumulative production of fractured well for year n [ft^3]

$N_{p.n}^{nf}$ forecasted annual incremental cumulative production of non-fractured well for year n [ft^3]

k' fluid consistency index [lb*s^n'/ft^2]

γ_n shear rate [1/s]

n' power law exponent

τ_y yield stress [lb/100 ft^2]

K fluid consistency index [lb/100 ft^2]

$\dot{\gamma}$ shear rate [RPM]

n power law index

τ_y yield stress [lb/100 ft^2]

θ_3 dial reading at 3 RPM [lb/100 ft^2]

θ_6 dial readings at 6 RPM [lb/100 ft^2]

k permeability [mD]

q flowrate [ft^3/s]

μ fluid viscosity [cP]

L length [ft]

ΔP pressure drop [psi]

A the cell cross section [ft^2]

P_{hydr} hydrostatic pressure of the fluid [psi]

$ISIP_{dh}$ bottomhole instantaneous shut in pressure [psi]

$ISIP_{wh.}$ instantaneous shut in pressure at surface [psi]

Δt_D dimensionless time function

dP/dG the first pressure derivative versus G

$\propto_a$ leakoff area parameter

$\propto_{c2}$ leakoff parameter during shut-in

g_0 computed value of G-function at shut-in

t shut-in time [hrs]

t_p pumping time [hrs]

σ_{prop} closure pressure acting on proppants [psi]

p_{wf} bottomhole well flowing pressure [psi]

References

[1] R. Nolen-Noeksema, “Elements of hydraulic fracturing,” *Oilfield review ,* pp. 51-52, 2013.

[2] J. Bellarby, Well completion design, Amsterdam: Elsevier B.V., 2009.

[3] M. T., “BJ Service's company hydraulic fracturing manual,” 2005.

[4] R. B. &. LLC, “Modeling fracture geometry,” 2009.

[5] B. Brady and J. e. al., “Cracking rock: progress in fracture treatment design,” *Oilfield Review,* pp. 4-17, 1992.

[6] K. G. N. Economides Michael J., Reservoir simulation, West Sussex: WILEY, 2000.

[7] B. &. Associates, “Gohfer user manual,” 2016.

[8] F. J., Hydraulic fracturing chemicals and fluids technology, Oxford: Elsevier Inc., 2013.

[9] Feng Li et. al (2016) A comprehensive review on proppant technologies, P.27

[10] Presentations from Professor Herbert Hofstaetter, Research Topics 2016 ff, Chair of petroleum & Geothermal Energy recovery, Mining University of Leoben.

[11] "Swarco industrial glass beads,” Swarco, [Online]. Available: https://www.swarco.com/northamerica/Products-Services/Glass-Beads/Industrial-Beads. [Accessed 01 08 2017].

[12] “Instruction Manual for Model 800 viscometer,” OFI testing equipment Inc., Houston, Texas, 2016.

[13] G. L. Boyun Guo, Applied Drilling Circulation systems, Oxford: Elsevier, 2001.

[14] A. P. Institute, “Recommended Practice for measurement of and specifications for proppants used in hydraulic fracturing and gravel-packing operations,” API standards department, Washington.

[15] N. M. L. O. e. Robert Duenckel, “The Science of proppant conductivity tetsing-Lessons learned and best practices,” *SPE,* p. 20, 2016.

[16] J. R. Robert R. McDaniel, “The effects of various proppants and proppant mixtures on fracture permeability SPE 7573,” p. 12, 1978.

[17] F. E. S. G. &. C. KG, “Lab report for Beer fluid and Swarco beads,” Salzwedel, 2016.

[18] F.E. Syfan, B.R.Meyer “Case history: G-function analysis proves benefcial in Barnett shale application SPE 110091” p. 10, 2007.

[19] "Pre-closure analysis introduction”, [Online]. Available: http://www.fekete.com/SAN/TheoryAndEquations/WellTestTheoryEquations/Pre-Closure_Analysis_Introduction.htm [Accessed 05 08 2017].

[20] R.V.Malpani, “Selection of fracturing fluid for stimulating tight gas reservoir,” Texas A&M University, 2016.

[21] P.A. Sookprasong, BJ Services, “In-situ closure stress on proppant in the fracture: a controversial new thinking SPE 136338,” p. 7, 2010.

List of Tables

List of Figures

Abbreviations

BEER®	Bio Enhanced Energy Recovery
GOHFER	Grid Oriented Hydraulic Fracture Extension Replicator
LOT	Leak-off test
XLOT	Extended leak-off test
FIT	Formation integrity test
OIP	Oil in Place
GIP	Gas in Place
LEFM	Linear Elastic Fracture Mechanism
PKN	Perkins-Kern-Nordgren
KZD	Kristianovich and Zheltov - Daneshy
NPV	Net Present Value
HPG	Hydroxapropyl guar
CMHPG	Carboxymethyl hydroxapropyl guar
HEC	Hydroxyethylcellulose
HPC	Hydropropylcellulose
ISP	Intermediate-strength proppant
LWC	Lightweight ceramics
IDC	Intermediate density ceramics
UHSP	Ultrahigh strength proppants
RCP	Resin-coated proppants
DFIT	Diagnostics Fracture Injection Test
PCA	Pre-closure analysis
ISIP	Instantaneous shut-in pressure
MD	Measured Depth
TVD	True Vertical Depth
GR	Gammy ray
RESIST	Resistivity
PHIN	Neutron porosity
RHOB	Bulk density
VSAND	Volume of sand
VSHALE	Volume of shale
VCOAL	Volume of coal
VLIME	Volume of limestone
VDOLO	Volume of dolomite
DTC	Compressional sonic wave time
PR	Poisson’s ratio
YMES	Young’s Modulus
PERM	Permeability
BHFP	Bottomhole flowing pressure